Equilibrium, Photophysical, Photochemical, and Quantum Chemical Examination of Anionic Mercury(II) Mono- and Bisporphyrins†

Zsolt Valicsek,*,‡ György Lendvay,*,‡,§ and Ottó Horváth‡

Department of General and Inorganic Chemistry, Institute of Chemistry, University of Pannonia, H-8201 Veszprém, P.O. Box 158, Hungary, and Institute of Structural Chemistry, Chemical Research Center, Hungarian Academy of Sciences, H-1525 Budapest, P.O. Box 17, Hungary

Received: May 7, 2008; Revised Manuscript Received: August 25, 2008

Mercury(II) ion and 5,10,15,20-tetrakis(parasulfonato-phenyl)porphyrin anion can form 1:1, 2:2, and 3:2 (metal ion/porphyrin) out-of-plane (OOP) complexes, from which $Hg_2P_2^{8-}$ has not been identified until now. Identification of this species significantly promoted the confirmation of the composition and the precise elucidation of the equilibrium of $Hg_3P_2^{6-}$. Since the formation of each complex is too fast, their kinetic behavior was studied from the side of dissociation. The rate-determining step in dissociations, as well as in the formation of the 2:2 complex, that is, the dimerization of 1:1 complex, proved to be virtually first-order under these conditions, while the consecutive formations of HgP^{4-} and $Hg_3P_2^{6-}$ are second-order reactions. The equilibria can be spectrophotometrically investigated because the Soret- as well as the Q-absorption bands of the free-base ligand are more and more red-shifted in the series of 1:1, 2:2, and 3:2 complexes, and the split of Q-bands disappears as the singlet-1 excited states become degenerate; in the case of bisporphyrins, the bands broaden, especially in the longer-wavelength region of the spectra. The quantum yield and the lifetime of S_1-fluorescence from the macrocycle is decreased by the insertion of a mercury(II) ion due to distortion, and in bisporphyrins the luminescence totally ceases because their more complicated structure promotes other ways of energy dissipation. The lifetime of the triplet excited-state is also reduced by metalation. The transient absorption measured upon excitation of $Hg_3P_2^{6-}$ probably originates from $Hg_2P_2^{8-}$ formed by efficient photodissocation during the laser pulse. This photoinduced dissociation is characteristic to out-of-plane complexes, but in metallo-monoporphyrins it needs the energetically higher Soret-excitation; in bisporphyrins, it can take place during irradiation at the longer Q-wavelengths. Investigation of the intramolecular photoredox reactions has proved that for the increased efficiency of the indirect photoinduced LMCT, not the redox potential, but the position of the metal center is responsible. The two orders of magnitude higher photoredux quantum yield for the 3:2 complex, compared to that of the 2:2 species, can be explained by the repulsive effect of the inner mercury(II) ion pushing the other two farther out of the ligand cavity. In bisporphyrins the second excited states are photochemically more reactive than the first ones, while most of the photochemical processes of HgP^{4-} originate from the first excited state. According to our quantum chemical calculations, the mercury(II) ion causes the expansion of the porphyrin-cavity; therefore its out-of-plane position is smaller than the value expected based on its ionic radius. In the hitherto unknown 2:2 dimer two 1:1 saucer-shaped monomers are kept together by secondary forces, mostly by $\pi-\pi$ interaction, but their relative arrangement was not unequivocally determined by the two DFT functionals used. The arrangements with a symmetry axis or plane perpendicular to both rings are not favored; instead, the two monomers are shifted along the porphyrin planes, either in a Hg−P−Hg−P or a Hg−P−P−Hg order. Our time-dependent density functional theory (TD-DFT) calculations indicate that the electronic spectra are not very sensitive to the structure of the dimer, even though the environment of the porphyrin rings is quite different if one of the metal ions is between or outside of both macrocycles. The calculated spectral shifts agree only partially with the experimental data. The TD-DFT calculations suggest that the chromophores are not fully independent in the bisporphyrins and that the observed spectral shift cannot be uniquely assigned to the geometrical distortion of the porphyrin macrocyle.

Introduction

Photochemical and photophysical features of metalloporphyrins are very important for understanding the mechanisms of numerous natural and artificial porphyrin-based catalytic and photosensitization phenomena. These properties are basically determined by the extensively conjugated electronic structure of the porphyrin ring as well as its geometry, localizing its four coordination sites in the center. For an extensive conjugation, planar structure is preferable. However, in porphyrins geometrical distortion can arise due to overcrowded peripheral substitution and special metalation, too,[1,2] because the size of the metal center is one of the most important factors influencing the geometry of porphyrin complexes.[3] Too short of a metal−nitrogen bond (significantly shorter than 2 Å) generally

† Part of the "Janos H. Fendler Memorial Issue".

* To whom correspondence should be addressed. (Z.V.) Phone: +36 (88) 624431. Fax: +36(88) 624548. E-mail: valicsek@vegic.uni-pannon.hu.(G.L.) Phone: +36 1 438 1124. Fax: +36 1 325 7554. E-mail: lendvay@chemres.hu.

‡ University of Pannonia.

§ Hungarian Academy of Sciences.

10.1021/jp804039s CCC: $40.75
Published on Web 10/28/2008

induces ruffle or saddle distortion of the porphyrin ring.[1,4−7] Conversely, if the bond is considerably longer than one-half of the diagonal N−N distance in the free-base porphyrin, dome deformation can take place.[4,6] This happens if the radius of the metal center exceeds the critical value of about 80 pm, or it does not prefer the square planar coordination. Such metal ions do not fit into the cavity of the ligand, and are located above the plane of the pyrrol-nitrogens, which also induces the out-of-plane distortion of the ring. The out-of-plane (OOP) complexes have been distinguished from in-plane metalloporphyrins since their discovery, at the beginning solely on the basis of complex stability as well as replaceability of the metal center.[8] They attracted greater attention when OOP complexes were identified as intermediates in the formation of in-plane metalloporphyrins. Such species, in which also the hydrogens remain connected to the pyrrol-nitrogens together with the partially coordinated metal ion, were the first complexes called as sitting-atop (SAT) metalloporphyrins.[9] If the metal center is not able to fit coplanar into the porphyrin cavity, even after the deprotonation of the ligand, these complexes are also named allo,[10] exoplanar,[11] sitting above the plane,[12] roof,[13] and dome[1] metalloporphyrins, but the SAT term has also been used for these final, relatively stable, out-of-plane products of complexation.[14−20] In order to avoid any misunderstanding in the rest of the paper, for such complexes we shall exclusively use the "out-of-plane" (OOP) term, and for planar complexes the notations shall be "in-plane" or "normal".

The out-of-plane metalloporphryins are thermodynamically less stable and kinetically more labile than the in-plane complexes, they are formed faster, and are more reactive.[8,18] The OOP complexes can be formed as intermediates in the catalytic production of the in-plane ones, so that a negligible quantity of a larger metal ion can accelerate the insertion of smaller ones by orders of magnitude. The mercury(II) ion was found to be a far more efficient catalyst in this respect than, for example, lead(II) or cadmium(II) ions.[8,21−28] Moreover, the OOP position of the metal center opens the possibility of aggregation in a special mode, because these complexes can be interconnected not only by head-to-tail (deck of card) interaction,[29−31] through a covalently bound peripheral bridge[32] or an additional ligand between the metal centers of two porphyrins,[33,34] but the out-of-plane metal ion can also be coordinated at the same time to the cavities of two macrocycles, resulting in the so-called sandwich structures.[35−40] Furthermore, in OOP metalloporphyrins the out-of-plane position of the metal center makes the charge separation via photoinduced charge-transfer from the ligand to the metal ion more efficient, which is often irreversible and allows their utilization for the cleavage of water[41] and as catalysts in the syntheses of chemicals suitable for conservation of light energy.[42]

We found that the absorption, photophysical and photochemical features of several OOP complexes are very similar, such as those of the typical OOP-complex mercury(II),[15,18] mercury(I),[18,43] and thallium(I)[16,18] porphyrins, the secondary conformers of cadmium(II) and lead(II) porphyrins,[43] and the complexes at the borderline between normal and out-of-plane types as iron(II),[17,18,20] manganese(II), and zinc(II) porphyrins.[43] The similarity of the properties of OOP porphyrins containing metal centers with so widely varying electronic structure as well as chemical nature suggests that these properties are primarily determined not by the electronic structure of the metal ion but by the geometrical structure of the complex. The properties of in-plane metalloporphyrins vary much wider with the nature of the metal center. The probable reason for this is that in this geometrical arrangement the atomic orbitals of the metal center can efficiently overlap with the molecular orbitals of the macrocycle and can perturb their energy levels, the magnitude of which depends on the identity of the metal. This effect is reduced in out-of-plane complexes, resulting in more uniform behavior.[18,44,45]

In the practice of metalloporphyrin categorization, Gouterman's method[46] is generally used to explain the properties of OOP complexes. This theory derives the properties of metalloporphyrins exclusively from the electronic structure of metal ions. It should be noted, however, that the size of the metal center and the nature of the coordinative bond were found important in another categorization of metalloporphyrins proposed earlier by Barnes−Dorough.[8] In later studies, correlation was found between the position of the metal center, more precisely, the character of bonds and stereochemistry, as well as the spectroscopic behavior of the ligand.[47]

The overview of the existing experimental results concerning OOP metalloporphyrins indicates that our knowledge of the properties of this class of metalloporphyrins is incomplete, not only for the complexes of less investigated metal ions, but even for the model compounds, mercury(II) porphyrins, whose composition has not been established. The complexation between mercury(II) ion and porphyrin was utilized to detect this toxic heavy-metal ion also in very low concentration, not only by very sensitive techniques like potentiometry and liquid chromatography,[48] but also by spectrophotometric and fluorometric[48−52] methods. The latter two methods belong to the most fundamental techniques in porphyrin chemistry, also providing information about the electronic structure and thus the physicochemical properties.[53] The metalation of the ligand causes well characterizable changes in spectra.[46] According to our experience, the formation of in-plane metalloporphyrins generally induces hypsochrom shifts, while that of out-of-plane complexes result in a bathochrom effect in the absorption spectra.[15−20,43] Concerning this latter observation, the red shift of UV−vis $\pi-\pi^*$ bands was found to be the consequence of distortion, mainly in the case of peripheral substitution (so-called perturbed porphyrins)[1,54,55] and also if the pyrrol-nitrogens are alkylated.[56] The fluorometric consequence of deformation was observed as the decrease of quantum yield and lifetime of emission.[1,54−57] However, the role of the geometrical distortion of the macrocycle in inducing the bathochrom effect has not been unambiguously settled; some theoreticians found no direct connection between red shift and distortion,[58−64] others assume their role as one of the important factors[65] including IPNR (in the plane nuclear reorganization),[61] and many theoretical studies indicated that distortion does have a major role.[4,66−73] We will try to connect,[43] via analyzing the data on OOP metalloporphyrins, the two aspects that are generally used separately in the interpretation of the properties of metalloporphyrins; one is the consideration of the electronic structure of the metal center only, and the other is the separate study of the distortion of the porphyrin moiety due to substitution.

We do this by studying the composition, absorption and emission, equilibrium, and photochemical studies of the Hg^{2+}−porphyrin system. As we shall show, the existence of various compositions with varying distortion of the macrocycle makes this system a promising source of information on structure−property correlations. We have worked with water-soluble ionic porphyrins[74] as ligands, because in this way, the complexation can be studied quite simply but in more detail.[75] Also, the photochemical features are not disturbed by organic solvents. In addition, these porphyrins are able to photochemi-

cally cleave water molecules,[76−78] which may be applied for utilization of solar energy. The tetrakis(parasulfonato-phenyl)porphyrin anion (H_2TSPP^{4-}) was used, because its negative charge can promote the coordination of the metal ion, and this electronic factor may increase the efficiency of photoinduced charge transfer processes.[78] Moreover, this anionic ligand is applied most widely for analytical purposes,[48] in photodynamic therapy,[79,80] in modeling of heme (in cyclodextrin),[81] and as MRI contrast agents.[82−84]

The main goal of our experimental and theoretical study was to investigate the formation, composition, electronic spectra, and photoinduced properties of the complexes in the H_2TSPP^{4-} $-Hg^{2+}$ system in order to explain the origin of the OOP features in these particular cases and generally to contribute to the elucidation of this type of behavior.

Methods

Materials and Methods. The analytical grade reagents, 5,10,15,20-tetrakis(parasulfonato-phenyl)porphyrin sodium salt ($H_2TSPPNa_4$), $C_{44}H_{26}N_4O_{12}S_4Na_4 \cdot 12H_2O$, and $Hg^{II}(ClO_4)_2 \cdot 3H_2O$ were purchased from Sigma-Aldrich and dissolved in deionized, double-distilled water purified with a Millipore Milli-Q system. The experiments were carried out at room temperature at pH = 7 and atmospheric pressure. The elimination of oxygen was ensured by argon bubbling and the Schlenk technique. The pH was set using a 0.01 M phosphate buffer, which also ensured that the ionic strength was $I = 0.02224$ M in all solutions. The pH = 7 was selected because at lower pH the hydrolysis of mercury(II) ions could cause the protonation of the H_2TSPP^{4-} (hereinafter H_2P^{4-}) anion ($pK_3 = pK_4 = 4.8$,[74] $pK_3 = 4.95$, and $pK_4 = 4.86$,[85] or $pK_3 = 4.99$ and $pK_4 = 4.76$[86]). The actual concentration of free-base ligand can be spectrophotometrically measured using the maximum of its Soret-absorption band at 413 nm ($\varepsilon_{max} = 5.10$,[85] 5.30,[87] 5.24,[88] or 4.66×10^5 $M^{-1}cm^{-1}$ [89]). We used the latest value for the absorption coefficent as it agrees with our own measurements. The molar extinction coefficients and the stability constants of mercury(II) porphyrins were simultaneously determined according to eqs 1−3

$$yH_2P^{4-} + xHg^{2+} \Leftrightarrow Hg_xP_y^{(2x-6y)} + 2yH^+ \qquad (1)$$

$$\beta_j' = \frac{\beta_j}{[H^{+2y}} = \frac{[Hg_xP_y^{(2x-6y)}]}{[H_2P^{4-}]^y[H^{2+x}} \qquad (2)$$

$$A_\lambda = l\sum_{j=1}^{n} \varepsilon_{j\lambda}\beta_j' \prod_{i=1}^{k} [c_i]^{\alpha_{ji}} \qquad (3)$$

by fitting the calculated absorption spectra to the measured ones using MS Excel. While for simple systems Excel proved to be reliable, more complicated titrations were evaluated by another program, PSEQUAD,[90−92] which uses the Newton−Raphson method for fitting the spectra. In every case, the number of species in the spectrophotometric titrations (or kinetic measurements) was determined using matrix rank analysis (with the code MRA[93]).

The apparent stability constants (β_j' in eqs 1 and 2) include the concentration of protons. The possible dissociation of axial ligands of the mercury(II) ion (for example, OH^-) is not included explicitely because their influence on the equilibria, in which we are interested in, is constant as all conditions (pH, ion strength, the nature of counter-ions) are kept the same in all solutions. The equilibrium constants β_j themselves can be calculated from the constant parameters.

The kinetics was described for the initial period of measured data mainly as second-order process in consecutive formation and first-order in dissociation of complexes,[19] but the reliability of these results was checked for the whole equilibrial complexation by a special software based upon Gauss−Newton−Marquardt method (ZITA[94]).

Instruments and Procedures. The absorption spectra were recorded and the photometric titrations were monitored using a single-beam GBC UV/vis 911-A and a SPECORD S-100 diode array spectrophotometer. The latter was also used for the determination of formation kinetics. For the measurement of fluorescence and excitation spectra a Perkin ELMER LS 50-B spectrofluorimeter was applied. The spectrum analyses were carried out by fitting Gaussian and Lorentzian curves in MS Excel. The second and third overtones of a Quantel Brilliant Nd:YAG laser with Phillips PM 3320/A or Tektronix TDS 684 A digital oscilloscopes served to investigate the excited states by time-resolved methods.[95] Since the fluorescence lifetime of porphyrins is comparable with the laser half-width, a convolution method[96] with three parameters was developed.[43] A series of LEDs was applied to record the transient absorption spectra in the 410−530 nm range. Unfortunately, due the low sensitivity of the apparatus outside this range we were not able to record the $T_1 \rightarrow T_2$ absorption bands. The $T_1 \rightarrow T_3$ molar extinction coefficients were determined by the method of inner standards from bleaching of ground-state absorption. The quenching rate constant with oxygen was determined from the lifetime difference between air-saturated and deaerated solutions.[97] For photochemical reactions under continuous irradiation, an AMKO LTI photolysis equipment, containing a 200 W Xe−Hg-lamp and a monochromator, was used,[95] and the light intensity of which was measured by ferrioxalate actinometry for the cuvettes with given optical length at several wavelengths from which the actual parameters were extrapolated.[95,98] For more accurate determination of photochemical quantum yields, an interlocked procedure was developed from the method of initial slope.[43]

Electronic Structure Calculations. The molecular geometries of metalloporphyrins were calculated using density functional theory (DFT).[99−102] The B3LYP[103−105] combination of functionals as well as the M05 functional proposed recently by Truhlar and co-workers[106,107] was used, together with the Hay−Wadt valence double-ζ (LANL2DZ) basis set which includes the influence of the inner-shell electrons on the valence shell using effective core potentials (ECP) for heavy-metal ions were applied.[108−111] The B3LYP/LANL2DZ combination was found to be efficient for the description of porphyrins in the literature,[112−114] in the present system we found, however, that it is not the most suitable method to characterize the $\pi-\pi$ interaction in Hg_2P_2 complex. The M05/LANDL2DZ combination seems to be more satisfactory for that purpose.

Most of our electronic structure calculations were performed using the unsubstituted porphyrin, $H_2P = C_{20}H_{14}N_4$. Electronic spectra of the complexes were also calculated using time dependent DFT.[115−117] All calculations were performed using the Gaussian 03 suite of programs.[118]

Results and Discussion

Equilibrium Constants. In contrast to organic solvents, where Adler's general recipe is used for the production of metalloporphyrins,[119,120] in water they are formed spontaneously in equilibrium processes.[21−24,27,75,121−126] Under ambient conditions the reaction takes place in reasonable time, or if not, it

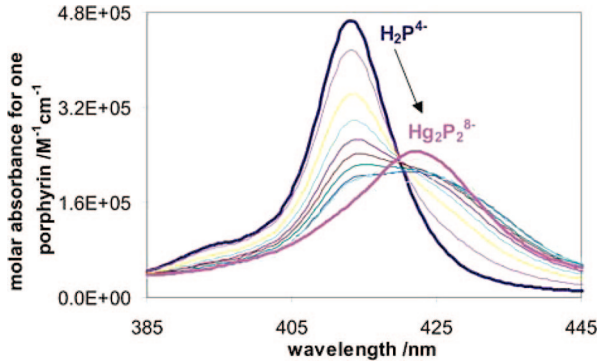

Figure 1. Spectrophotometric titration of 2.3×10^{-6} M H_2P^{4-} with mercury(II) ion in the concentration in the $0-1.3 \times 10^{-4}$ M range. The thick purple line represents the calculated molar spectrum of $Hg_2P_2^{8-}$ (referred to one porphyrin unit) at the Soret-band.

can be promoted with another metal ion.[8,21−28] The mercury(II) ion with 102 pm radius[127] forms in equilibrial reactions the typical OOP complexes with different composition: HgP (1 metal ion:1 porphyrin), Hg_2P_2 (2:2), Hg_3P_2 (3:2) and maybe Hg_2P (2:1) (the latter was proved not to exist in our experiments).[15,18] One axial (e.g., hydroxo) ligand can remain on the metal center. The other side of the distorted porphyrin core can weekly coordinate one water molecule but not more,[35] which is forced away in bisporphyrins.

The formation of the 1:1 complex, HgP^{4-}, can be observed only at very low porphyrin concentration (lower than 10^{-6} M). The isosbestic and isostilbic points presented in ref 15 during spectrophotometric titration proves that Hg_2P^{2-} is not formed at the highest mercury(II) ion concentration (below 10^{-2} M) in the presence of the applied phosphate buffer. The apparent stability constant determined for HgP^{4-} is $\beta_1' = (8.8 \pm 0.7) \times 10^5$ M^{-1} ($\lg\beta_1' \approx 5.95$),[15] which is in accordance with the only published result $\lg\beta_1' = 5.62$ (converted to pH = 7 from the reported $\lg\beta_1 = -8.38$).[128] The absorbance of the complex determined in ref 128 was smaller than that for the free-base ligand because the dimerization, that is, the formation of $Hg_2P_2^{8-}$ was not taken into consideration. In the literature, formation of a complex with such a constitution has not been reported; however, a hint indicating its existence can be seen in the photometric titration curves presented in ref 89 The difficulty of the spectrophotometric study of this species is that the position of its Soret-band ($\lambda = 422$ nm) just slightly differs from that of the HgP^{4-} complex (420.5 nm), thus they can not be distinguished, even by matrix rank analysis. At the Q-bands, on the other hand, they are distinguishable. If the photometric titration is carried out at higher porphyrin concentration (above 10^{-6} M), only a quasi isosbestic point can be obtained (Figure 1.), because more than two light-absorbing species exist in each solution: in addition to the 2:2 complex, at lower mercury(II) ion concentration the 1:1 complex is present in a considerable amount, while at higher concentration the 3:2 complex.

The apparent stability constant was determined: $\beta_{2:2}' = (5.6 \pm 0.5) \times 10^{14}$ M^{-3} ($\lg\beta_{2:2}' \approx 14.75$), from which the real dimerization constant is found to be $K_{2:2} = (7.2 \pm 0.6) \times 10^2$ M^{-1} ($\lg K_{2:2} \approx 2.86$).[18]

In most papers on mercury(II) [tetrakis-(4-sulfonatophenyl)porphyrin] complexes, a species displaying a Soret-band at about 435 nm was discussed, but its composition has not been unambiguously determined; metal-to-porphyrin ratios of 2:1[24,26,89,126,129−131] and 3:2[128] have been proposed. Nahar and Tabata[131] proved that the 2:1 complex, if at all, could exist only in the narrow pH range of 2.5−4. Trimercury(II)-bisporphyrins were well known beforehand,[35,36] especially in the case of tetraphenyl-porphyrins.[132] Adeyemo and

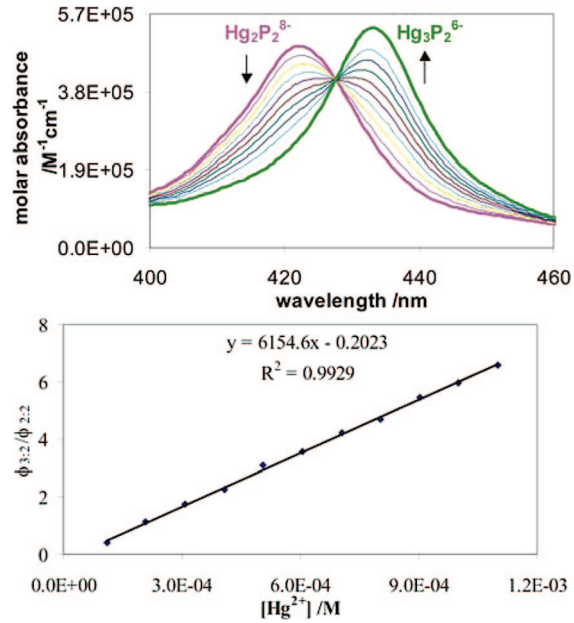

Figure 2. Spectrophotometric titration of 5.0×10^{-6} M H_2P^{4-} with mercury(II) ion in the $1.1 \times 10^{-4} - 1.1 \times 10^{-3}$ M concentration range, and the ratio of the partial molar fractions of these two complexes vs the free mercury(II) ion concentration. The thick purple line represents the calculated molar spectrum of $Hg_2P_2^{8-}$ and the green that of $Hg_3P_2^{6-}$.

Krishnamurthy spectrophotometrically investigated the equilibrium in aqueous solution and found a species that they first considered as Hg_2P^{4-}.[129] Later, in a reinvestigation of the equilibrium, they found that at lower porphyrin concentrations than in their previous study, the composition of the complex is 1:1, and at high porphyrin concentration it is 3:2 (what they earlier thought to be 2:1).[128] While these authors presented titration curves for formation of $Hg_3P_2^{6-}$ from free-base porphyrin which shows a well defined isosbestic point, Tabata and Ozutsumi[89] found that the isosbestic point is blurred, which they considered a spectral anomaly. Our measurements show that this phenomenon is caused by the formation of $Hg_2P_2^{8-}$.

Our spectrophotometric titration is shown in Figure 2 and evaluated according to eqs 4−6:

$$Hg^{II}{}_2P_2^{8-} + Hg^{2+} \leftrightarrow Hg^{II}{}_3P_2^{6-} \qquad K_{3:2}' = \frac{[Hg^{II}{}_3P_2^{6-}]}{[Hg^{II}{}_2P_2^{8-}]\,[Hg^{2+}]} \quad (4)$$

$$\varphi_{3:2} = \frac{2\beta_{3.2}'[Hg^{2+}]^3[H_2P^{4-}]}{1 + K_1'[Hg^{2+}] + 2\beta_{2:2}'[Hg^{2+}]^2[H_2P^{4-}] + 2\beta_{3:2}'[Hg^{2+}]^2[H_2P^{4-}]} \approx \frac{K_{3:2}'[Hg^{2+}]}{1 + K_{3:2}'[Hg^{2+}]} \quad (5)$$

$$\frac{\varphi_{3:2}}{\varphi_{2:2}} = K_{3:2}'[Hg^{2+}] \quad (6)$$

indicates that the 3:2 complex can be formed from the 2:2 species through a clear isosbestic point, which is in accordance with eq 6. On the basis of this we can conclude that the spectrophotometric titrations indicate the existence of complexes

of composition 1:1, 2:2, and 3:2. To obtain the equilibrium constant, we note that eq 5 can be simplified because the partial molar fractions of free-base porphyrin and the HgP^{4-} complex are negligible as can be seen in Figure 2. As eq 6 is valid even without this simplification, the apparent consecutive formation constant is $K_{3:2}' = (6.2 \pm 0.5) \times 10^3\ M^{-1}$ ($\lg K_{3:2}' \approx 3.79$) from which the overall stability constant is $\beta_{3:2}' = (3.4 \pm 0.3) \times 10^{18}\ M^{-4}$ ($\lg \beta_{3:2}' \approx 18.54$).[18] This value is about 3 orders of magnitude higher than the only available value for this composition, $\lg \beta_{3:2}' = 14.3-15.5$ (converted from $p\beta_{3:2} = 12.5-13.7$) which was obtained without the knowledge of the existence of the 2:2 complex (the ignorance of the latter induces the large error bar and the strong wavelength dependence of the determination in ref 128).

Formation Kinetics. The mechanism of insertion of metal ions into the porphyrin ring is quite complicated.[135] On the time-scale of seconds the rate-determining step in water is generally associative and first order for both reagents.[19,43] Note that the intermediates H_2−P-M, (which Fleischer[9] originally called SAT complexes) are very short-lived, can be detected only in aprotic solvents,[9,121,136] but even then only with certain metal ions (not with the mercury(II) ion we are interested in[9]). The association step Hg^{2+} + free-base ligand was found to be too fast to be accurately measured.[124,137] The reverse reaction, the dissociation of metalloporphyrins can be studied more fruitfully (note that the reaction is 10^6 times slower than decomposition of complexes with noncyclic ligands[138]). Among metalloporphyrins the out-of-plane complexes (e.g., the mercury(II) porphyrins) are kinetically labile,[18,22] that is, their dissociation is relatively fast as compared to the in-plane ones. Their decomposition rate constant is the following:

$$-\frac{d[Hg_xP_y^{(2x-6y)}]}{dt} = k_-[Hg_xP_y^{(2x-6y)}] \quad (7)$$

$$k_- t = \ln \frac{[Hg_xP_y^{(2x-6y)}]_0}{[Hg_xP_y^{(2x-6y)}]} \quad (8)$$

$$K_i' \approx \frac{k_+'}{k_-} \quad (9)$$

is in the range that can be measured by the dilution method.[19,43] We determined the dissociation rate of the 2:2 complex using essentially this method. The formation and decomposition of the 1:1 complex, however, always proceeds in the presence and concomitant formation/decomposition of $Hg_2P_2^{8-}$, and the corresponding rate constant can be derived from indirect experiments. Figure 3 shows kinetic curves measured at low porphyrin concentrations. One can see that the formation of HgP^{4-} is always accompanied by the appearance of $Hg_2P_2^{8-}$ even at very small, but still measurable porphyrin concentrations. From the concentration change in the initial period we derived for the first-order dissociation constant of the dimer (the 2:2 complex) the value $k_{2:2-} = (3.5 \pm 0.4) \times 10^{-3}\ s^{-1}$, from which the dimerization constant may be estimated: $k_{2:2+}' \approx K_{2:2}' \times k_{2:2-} \approx 2.5 \pm 0.3\ s^{-1}(M^{-1})$ (eq 9).

Figure 4 shows the kinetic curves obtained if the concentration of porphyrin is higher than, and the mercury(II) concentration is the same as in Figure 3. At these conditions, the 2:2 species is essentially the only initial product (the presence of monomer is negligible). The time dependence of its concentration can be

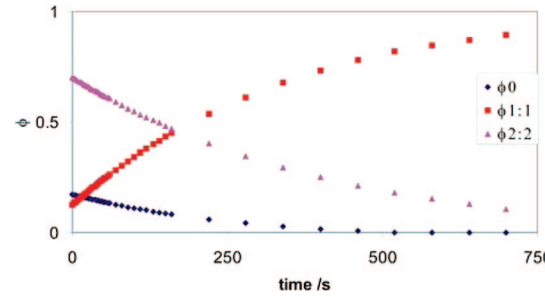

Figure 3. The change of partial molar fractions of porphyrin species as a function of time (starting within one minute after mixing of diluted reagent solutions) at 1.3×10^{-7} M porphyrin and 7.4×10^{-5} M mercury(II) concentration. Diamonds, H_2P^{4-}; squares, HgP^{2-}; triangles, $Hg_2P_2^{6-}$.

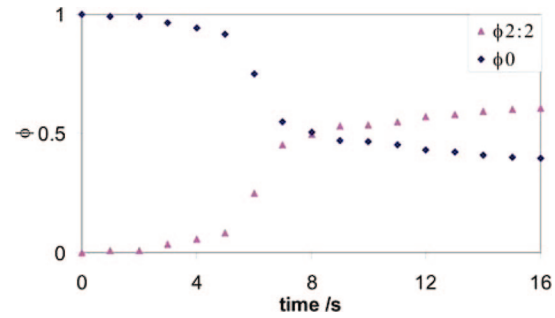

Figure 4. Partial molar fractions vs time at 2.6×10^{-6} M porphyrin and 8.2×10^{-5} M mercury(II) concentration. Diamonds, H_2P^{4-}; triangles, $Hg_2P_2^{6-}$.

obtained from the reaction scheme in eq 10 according to eq 11

$$Hg^{2+} + H_2P^{4-} \overset{k_{1:1+}'}{\longleftrightarrow} HgP^{4-} \overset{k_{2:2+}'}{\longleftrightarrow} \frac{1}{2}Hg_2P_2^{8-} \quad (10)$$

$$[Hg_2P_2^{8-}] = [H_2P^{4-}]_0 \times \left(1 + \frac{k_{2:2+}' \exp(-k_{1:1+}'[Hg^{2+}]t) - k_{1:1+}'[Hg^{2+}]\exp(-k_{2:2+}'t)}{k_{1:1+}'[Hg^{2+}] - k_{2:2+}'}\right) \quad (11)$$

The unidirectional formation of $Hg_2P_2^{8-}$ was barely followable on the time-scale of seconds, but from the evaluation of several experiments containing different reagent concentrations, the rate-determining step of dimerization seemed to be a first-order process (eqs 10 and 11; $k_{2:2+}' \approx 2.5 \pm 0.3\ s^{-1}$), that is, not the association of monomers, rather, a subsequent change in the structure of this intermediate dimer is the slowest step. On the basis of this observation, the formation constant of the monomer can be approximately calculated from the kinetic curves in Figure 4: $k_{1:1+}' = 790 \pm 80\ M^{-1}s^{-1}$, from which the dissociation rate constant may be estimated to be $k_{1:1-} \approx k_{1:1+}'/K_1' \approx (8.9 \pm 0.9) \times 10^{-4}\ s^{-1}$ (applying our simplifications for pH = 7, where no acid-induced dissociation occurs, deviating from the observation by Hudson and Smith[139] on HgTPP:

2 HgTPP + 2 HCl → H_2TPP + ClHg-TPP-HgCl (+ 2 HCl) → 2 H_2TPP + 2 $HgCl_2$)

The formation of the 3:2 species from the dimer is very fast (at the time-resolution limit of our instrument), therefore for this reaction again the dissociation constant was measured. We obtained $k_{3:2-} = (4.9 \pm 0.5) \times 10^{-2}\ s^{-1}$, from which the consecutive formation constant could be estimated: $k_{3:2+}' \approx K_{3:2}' \times k_{3:2-} \approx 300 \pm 40\ M^{-1}s^{-1}$.

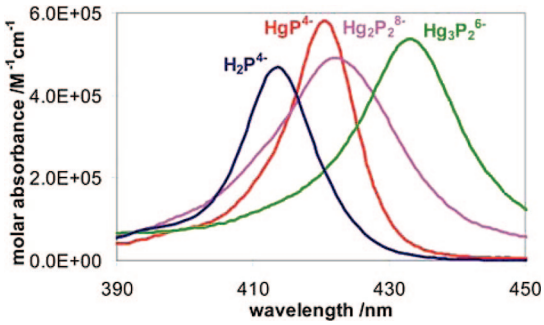

Figure 5. Molar absorption spectra of mercury(II) porphyrins at the B-band.[18]

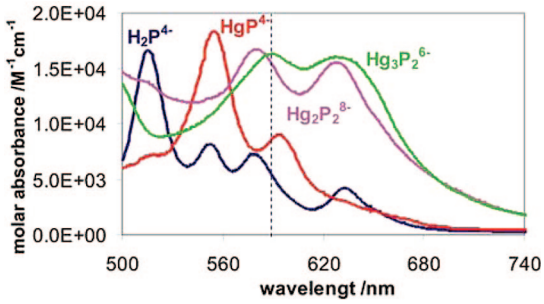

Figure 6. Molar absorption spectra of mercury(II) porphyrins at the Q-bands (the dotted blue line represents the average energy of $Q_y(0,0)$ and $Q_x(0,0)$ of free-base porphyrin).

Absorption Spectra. The absorption spectra of free-base porphyrin and the three Hg^{II}-porphyrin complexes presented in Figures 5 and 6 show that the formation of mercury(II) porphyrins from free-base porphyrin, as typical for out-of-plane complexes, is accompanied by a bathochrom effect. The magnitude of the shift increases with the complexity of the molecule in both the Soret-[18] (Figure 5 and Table 1) and the Q-region (Figure 6 and Table 2) of visible spectra. The band shifts refer to the Soret- or B(0,0) and the Q(0,0) transitions, where the first number in parentheses denotes the vibrational quantum number of the excited (the S_2 and S_1 states, respectively), the second that of the ground electronic state.[78,87] The determination of the magnitude of the red shift is complicated by the fact that the presence of H atoms in free-base porphyrin reduces the symmetry ($D_{4h} \rightarrow D_{2h}$) and splits the Q-band ($Q \rightarrow Q_x + Q_y$),[140] therefore there are five bands in this spectral region of free-base-, in contrast to three in those of metalloporphyrins[141] (Table 2.). As Gouterman suggested,[142] the shift is calculated with respect to the average energy of $Q_x(0,0)$ and $Q_y(0,0)$ bands of free-base porphyrin (note that in our earlier papers[15−20] we have not yet use this convention).

The Soret maximum of the previously unidentified $Hg_2P_2^{8-}$ dimer, as mentioned above, is very close to that of the monomer, 423 versus 420 nm, according to spectrum analysis. On the other hand, the Q-band maxima, 579 and 629 nm, are closer to those of the 3:2 complex, 585 and 640 nm, respectively. The appearance of the absorption red shift in heavy-metal porphyrins can be explained by recalling that the metal orbitals are closer in energy to the antibonding π^* molecular orbitals (lowest unoccupied molecular orbitals, LUMOs) than to the binding π orbitals (highest occupied molecular orbital, HOMO) of porphyrin, so that the perturbation they cause decreases the energy of the LUMOs more than that of the HOMO, resulting in the bathochrom effect of $\pi\pi^*$ transitions. Accordingly, the observation that the Soret band of the 2:2 complex is closer to that of the monomer can be explained by assuming that the metal ion strongly polarizes the delocalized electron system, influencing the higher-energy, $S_0 \rightarrow S_2$ absorptions. The Q-band of the 2:2 complex is closer to that of the 3:2 complex probably because the longer-wavelength, $S_0 \rightarrow S_1$ transitions are influenced more by the $\pi-\pi$ interaction between the porphyrin rings.

We found that the molar absorption coefficients of HgP^{4-} (at band maxima) are larger than for free-base porphyrin (Tables 1 and 2). Note that the opposite tendency,[128] reported at slightly higher porphyrin concentrations is virtual: partial dimerization of HgP^{4-} takes place and the absorption coefficient of the dimer is essentially the same as that of the monomer. The inspection of data in Tables 1 and 2 indicates that the molar absorption coefficient of the 3:2 complex is larger than that of the monomer. At the strongest absorption bands $Hg_3P_2^{6-}$ absorbs almost twice as efficiently as the monomer, which suggests that the two porphyrin chromophores are independent. Exceptions are the B(0,0) and Q(1,0) bands where the molar absorption coefficient of the monomer is somewhat larger than that of the 3:2 complex, but, because the bands are broader in the 3:2 complex, the oscillator strength is much larger in the latter at these absorptions, too. This band broadening may be caused in part by merging of bands.[80] Another factor for enhanced absorption ability is a possible appearance of new bands.[40,143] In the spectra we obtained for Hg(II) bisporphyrins, no separate new bands can be seen.

The tendencies seen in the present work are in agreement with those observed for other out-of-plane complexes, which were found to absorb light more efficiently than the free-base ligands or the normal metalloporphyrins;[18,43] hence, they could be more efficient in optical sensors and harvesting of light energy for artificial photosynthesis.

A closer look at the band intensities shows that the oscillator strengths and the vibronic splittings of the 2:2 complex are very similar to those of the 3:2 complex, instead of the 1:1 complex, even at the Soret band, the location of which showed the opposite tendency. From this observation, we conclude that the two porphyrin chromophores, from the viewpoint of absorption intensity, are independent from each other in both bisporphyrins. Their interaction is manifested in a band broadening, probably due to $\pi-\pi$ interactions. The deviation in the band shifts is presumably a consequence of the different local environment in the 3:2 and 2:2 complex.

The $\pi-\pi$ interactions were thoroughly studied in the case of dimerization and aggregation of free-base porphyrins, and the results indicate that the twist of aryl substituents minimizes the repulsion and maximizes the stacking $\pi-\pi$ interaction of ionic porphyrins−hydrophobic aryls interlock to exclude the water molecules.[4,29−31,144] The pH, the ionic strength, and the nature of substituents influence the dimerization of HgP^{4-} probably in the same way as in the case of the aggregation of free-base or protonated porphyrins. Such processes are more characteristic to anionic ligands, because their substituents with negative charge can bind more probably to the positive cavities.[29−31] The aggregation can make the investigation of equilibria more difficult, but it significantly occurs only over $I = 1$ M ionic strength[145] (at overall porphyrin concentration of 3.12×10^{-5} M the concentration of the monomer and the dimer are equal, $[H_2P^{4-}] = [(H_2P)_2^{8-}] = 1.04 \times 10^{-5}$ M as $K_D = 9.6 \times 10^4$ M^{-1}).[125] It was observed that the tetrasulfonato species ($H_2TPPS_4^{4-}$) is not susceptible to aggregation except above 10^{-3} M, deviating from the trisulfonato derivative ($H_2TPPS_3^{3-}$), which as byproduct of direct sulfonation is always present.[87]

The $\pi-\pi$ interactions binding together the monomers can be spectrophotometrically examined by studying the broadening

TABLE 1: The Soret-Absorption Data of Free-Base and Mercury(II) Porphyrins[a]

species	H_2P^{4-}	HgP^{4-}	$Hg_2P_2^{8-}$	$Hg_3P_2^{6-}$
λ (B(1,0))/nm	395	400	400	410
ε_{max} (B(1,0))/10^4 M^{-1} cm^{-1}	8.09	7.34	11.27	11.54
λ_{Gauss} (B(1,0))/nm	396	406	403	412
ε_{Gauss} (B(1,0))/10^4 $M^{-1}cm^{-1}$	8.13	10.40	10.57	12.17
$\omega_{1/2}$ (B(1,0))/cm^{-1}	1149	1370	1593	1379
f (B(1,0))	0.361	0.550	0.642	0.649
ν (B(1,0))/cm^{-1}	1090	824	1184	1184
λ (B(0,0) /nm	413	421	422	433
ε_{max} (B(0,0))/10^5 $M^{-1}cm^{-1}$	4.66	5.62	4.91	5.37
λ_{Gauss} (B(0,0))/nm	414	420	423	433
ε_{Gauss} (B(0,0)) /10^5 $M^{-1}cm^{-1}$	4.45	5.09	4.53	5.07
$\omega_{1/2}$ (B(0,0)) /cm^{-1}	785	663	1198	977
f (B(0,0))	1.351	1.306	2.098	1.915
B-shift /cm^{-1}		−377	−522	−1090

[a] λ, measured wavelength; λ_{Gauss}, wavelength from spectrum analysis; $\omega_{1/2}$, halfwidth; *f*, oscillator strength; ν, energy of vibronic overtone.

TABLE 2: Q-Absorption Data of Free-Base and Mercury(II) Porphyrins; for Notations See Table 1

species	H_2P^{4-} *y*	H_2P^{4-} *x*	HgP^{4-}	$Hg_2P_2^{8-}$	$Hg_3P_2^{6-}$
λ (Q(2,0))/nm	490		518	540	540
ε_{max} (Q(2,0))/$M^{-1}cm^{-1}$	3347		5720	11915	9490
λ_{Gauss} (Q(2,0))/nm	489		515	541	528
ε_{Gauss} (Q(2,0))/$M^{-1}cm^{-1}$	3167		5736	11890	8602
$\omega_{1/2}$ (Q(2,0))/cm^{-1}	1121		1404	1512	2042
f (Q(2,0))	0.0137		0.0311	0.0695	0.0677
ν (Q(2,0))/cm^{-1}	1080		1372	1214	1846
λ (Q(1,0))/nm	516	579	556	580	590
ε_{max} (Q(1,0))/$M^{-1}cm^{-1}$	16657	6669	18365	16740	16295
λ_{Gauss} (Q(1,0)) /nm	517	582	554	579	585
ε_{Gauss} (Q(1,0))/$M^{-1}cm^{-1}$	16062	6155	17320	12591	14105
$\omega_{1/2}$ (Q(1,0))/cm^{-1}	827	846	967	1021	1685
f (Q(1,0))	0.0513	0.0201	0.0648	0.0497	0.0919
ν (Q(1,0))/cm^{-1}	1180	1385	1216	1374	1467
λ (Q(0,0))/nm/	553	633	594	628	628
ε_{max} (Q(0,0))/$M^{-1}cm^{-1}$	6985	3980	7694	15548	16016
λ_{Gauss} (Q(0,0)) /nm	550	633	594	629	640
ε_{gauss} (Q(0,0)) /$M^{-1}cm^{-1}$	6433	3676	7426	14856	13593
$\omega_{1/2}$ (Q(0,0)) /cm^{-1}	830	727	774	1651	1475
f (Q(0,0))	0.0206	0.0103	0.0222	0.0949	0.0775
Q-shift/cm^{-1}			−167	−1091	−1375
B-Q energy gap /cm^{-1}	7174		6964	7743	7460

and the shifts of absorption bands. Among the spectrophotometric consequences of dimerization as a kind of aggregation, the band shifts are hard to determine. In the literature, blue shift of Soret-band[40,143−149] and the simultaneous red shift of Q-bands[40,143−147] was reported; others observed bathochrom effects of both absorptions.[30,31,53,80] At the Soret-band we observed aggregation-induced blue shift for the free-base, but red shift for the mercury(II)- and the diprotonated porphyrins, while only bathochrom effect in the Q-region, the magnitude of which varied, similarly the change of intensity of vibronic overtones and the decrease of efficiency of fluorescence (see later). It seems that the change of the shape of the macrocycle from planar to deformed in the monomer units can result in different directions of shift of the Soret-band, but in the Q-range it modifies only the magnitude of the bathochrom effect. According to another interpretation, a charge-resonance state causes the bathochrom, while a dipole−dipole interaction the hypsochrom effect in cofacial dimers.[53]

Because of intensity borrowing, transitions to higher vibrational levels of the excited electronic states also appear in the spectra of porphyrins.[1,150] The frequencies of the vibronic overtones for the porphyrins we studied (ν in Tables 1 and 2) were derived from spectrum analysis (more accurately than directly from the measured spectra). The frequencies obtained for HgP^{4-} are a little smaller at the Soret-band and a little larger in the Q-region than for the free-base ligand, those for the bisporphyrins are larger at both bands.

The last row of Table 2 displays the energy gap between the B(0,0) and Q(0,0) bands, the value of which is almost constant, about 7000 cm^{-1}, for monoporphyrins.[43] The reason for this similarity may be that the metalation causes the same perturbation on the S_1- and S_2-states of the ligand. The energy gap increases in bisporphyrins because their red shifts are larger in their Q-region than at the Soret-band, contrary to monoporphyrins. This phenomenon can be attributed to the $\pi-\pi$ interaction between two macrocycles.

Photophysics. Luminescence and nonradiative decay of porphyrins,[154] beside their biological importance, show very interesing features. Only a negligible part of excitation energy is lost via heat dissipation from singlet states, because the overall quantum yield of fluorescence and intersystem crossing resulting in formation of triplet states is over 95%, which is the major reason that makes porphyrins efficient in optical sensations and photosensitizations.[78]

The fluorescence spectra of HgP^{4-} and the free-base porphyrin are compared in Figure 7. The analysis of the spectra reveals the hitherto unknown Q(0,2) fluorescence band (Table 3 and Figure 7), which is the counterpart of the Q(2,0) absorption band

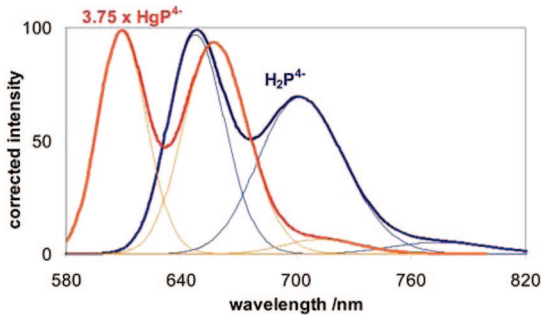

Figure 7. The analyzed S_1-fluorescence spectrum of HgP^{4-} compared with that of H_2P^{4-}.

and is just a little bit weaker. Metalation of the porphyrin induces a hypsochrom effect in the fluorescence: the (0,0) band is shifted by almost 1000 cm^{-1} (Table 3), in contrast to the red shift of absorption. Note that this blue shift−red shift anomaly is virtual, because the absorption shift is referred to the average of $Q_y(0,0)$ and $Q_x(0,0)$ bands of the free-base ligand, whereas the emission comes not from a hypothetical average level, but from the energetically lower S_{1x}-state (populated in $Q_x(0,0)$ absorption). The shift of the Q(0,0) transition ($Q_x(0,0)$ in the case of H_2P^{4-}) between absorption and emission, that is, the S_1 Stokes-shift characterizes the magnitude of the structural change during excitation. The Stokes shift is somewhat larger in HgP^{4-} than in H_2P^{4-}, although the complex is highly nonplanar already in the ground state, while the free-base ligand is planar. From this observation some information about the excited-state geometry can be obtained. For this we note that monoporphyrin complexes of many different metal ions were found to have very similar vibronic overtones (ν_1 is about 1200 cm^{-1} almost independently of the nature of the metal ion),[43] so in the S_1-excited-state these metalloporphyrins can be assumed to have the same degree of ring deformation. On the basis of this assumption, from the relatively large Stokes-shift for HgP^{4-} one can infer that in the ground state, although it is nonplanar, this complex is farther from the assumed "common" excited-state geometry. The latter is possibly even more nonplanar based on the observation that thallium(III) porphyrin, which in the ground state is farther from being planar than HgP^{4-}, has a smaller Stokes-shift (242 cm^{-1}).[19,43]

As Table 3 shows, both the quantum yield and the lifetime of S_1-fluorescence decreases due to the coordination of mercury(II) ion to the ligand., the former by a factor of 3, the latter by a factor of 4. The lifetime of the free-base ligand is 10 ns according to our measurement, which is similar to the published data for H_2TPP: τ_{S1} = 16,[154] 13.6,[151] 10.4,[87] and 12.4 ns.[152] While no literature value is available for the lifetime of fluorescence of HgP^{4-}, τ_{S1} = 2.7 ns which we obtain is very close to those of other out-of-plane porphyrins with Soret-absorption maximum at 421 nm.[43] It is known that the yield of fluorescence decreases if the symmetry of a structure is reduced,[53] and also that the efficiency of nonradiative decay increases with the deformation, especially with the out-of-plane position of metal center.[153] The derivation of the rate constants of the radiative and nonradiative processes from the corresponding data for H_2P and HgP^{4-} indicates that this is the case in this system, too. k_r hardly changes when Hg^{2+} is coordinated to the porphyrin, and k_{nr} increases by a factor of 4. This means that in this complexation the acceleration of nonradiative decay is responsible for the reduction of the fluorescence lifetime and not the deceleration of the radiative process as assumed in the literature based on the expectation that k_r is twice as large[78,154] in metalloporphyrins than in the free-base ligand. The efficiency of spin-forbidden steps may increase at the expense of spin-allowed ones (like the internal conversion from S_2- to S_1-state) because of the possible S_2-T_2 intersystem crossing. Taking this into account, and recalling that the excited-state geometries of the metalloporphyrins can be similar, the observation that the fluorescence lifetimes are nearly independent of the nature of the metal center implies that it is probably the geometry that determines the balance of excited-state processes.

In search for fluorescence from the 2:2 and 3:2 complexes, we observed very weak luminescence from solutions where the dominant species is one of HgP^{4-}, $Hg_2P_2^{8-}$, and $Hg_3P_2^{6}$, respectively. We compared the absorption and excitation spectra of each solution. We found that the absorption and excitation spectra of HgP^{4-} are essentially identical. This proves that the fluorescence originates from this complex. The absorption and excitation spectra obtained from solutions containing mostly $Hg_2P_2^{8-}$ or $Hg_3P_2^{6-}$, however, do not agree. Furthermore, a negative Stokes-shift can be measured, which suggests that this luminescence comes not from the dominant but from some other species. The emission and excitation spectra measured in such solutions are the same as those of the monomer, so that we can conclude that the species producing the measured fluorescence spectrum is the 1:1 complex. From this, our conclusion is that the bisporphyrins do not fluoresce. A plausible explanation for the observed emission could be that the bisporphyrins photodissociate and produce the 1:1 complex and this is the source of the weak emission. However, considering that the bisporphyrins are present in equilibrium solutions which always contain HgP^{4-} as a minor species with negligible partial molar fraction, there is no reason to assume the occurrence of photodissociation. The lack of emission from the bisporphyrins is probably due to their more complicated structure, promoting more effective vibronic decays. In ref 151, the quantum yield of fluorescence of a solution of mercury(II) TPP with a 433 nm Soret-maximum was found to be smaller than 10^{-3}. On the basis of the facts we just discussed, we can see that the emission observed in those experiments is also from the 1:1 complex, which was present in low concentration at their Hg^{2+} and TPP concentrations although the nonemitting bisporphyrins dominated, which was not considered when the quantum yield was calculated. Similar may be the reason for the observation that the Hg^{2+} ion quenches so very efficiently the emission of porphyrin films: at the relatively high local porphyrin concentrations not the 1:1, but mostly a nonemitting complex is formed.[52]

In arylated porphyrins the fluorescence from the S_1-state manifests a relatively rare peculiarity: its spectrum is antisymmetric to that of the absorption.[155] One of the possible reasons for this phenomenon is the extension of delocalization by the twisting of aryl substituents from almost perpendicular orientation to the porphyrin plane to closer to planar, causing an alternating excited state.[67] The magnitude of such structural change is probably smaller in distorted porphyrins, where the torsion angle of the meso-aryl groups is smaller already in the ground-state than in planar porphyrins. This may be the reason for the smaller fluorescence vs absorption spectral antisymmetry,[43] as observed for HgP^{4-} (Figures 6 and 7. From Table 2, for H_2P $I_{max}(0,1)/I_{max}(0,0)$ is 0.71 in fluorescence while it would be 0.6 if the spectrum were totally antisymmetric to the absorption one from Table 2. The same numbers are 0.95 and 0.43, respectively, for HgP^{4-} from Table 3.) The mercury(II) ion with a closed-shell $[Xe]4f^{145}d^{10}$ electron configuration does not luminesce and does not really influence electronically the emission of ligands in its complexes,[156] consequently, it is probably the steric effect what is responsible for the change of

TABLE 3: The S_1-Fluorescence Data of HgP^{4-} Compared with Those of H_2P^{4-}[a]

species	H_2P^{4-}			HgP^{4-}		
transition	$S_1(0,0)$	$S_1(0,1)$	$S_1(0,2)$	$S_1(0,0)$	$S_1(0,1)$	$S_1(0,2)$
λ ($S_1(0,i)$) /nm	648	702	775	609	657	713
$I_{max}(0,i)/I_{max}(0,0)$		0.712	0.053		0.951	0.065
$\omega_{1/2}$ ($S_1(0,i)$) /cm^{-1}	828	1065	1005	804	907	913
ϕ ($S_1(0,i)$)	0.0315	0.0289	0.0020	0.0111	0.0120	0.0008
ν ($S_1(0,i)$) /cm^{-1}		1197	1342		1212	1188
S_1-Stokes /cm^{-1}		360			400	
S_1-shift/cm^{-1}					981	
$\phi(S_1)$		0.0753			0.0239	
$\Phi(S_1$-Qy)		0.0624				
$\Phi(S_1-B)$		0.0562			0.0164	
ϕ(IC $S_2 \rightarrow S_1$)		0.746			0.684	
$\tau(S_1)$/ns		10.03			2.65	
$k_r(S_1)/10^6$ s^{-1}		7.51			9.02	
$k_{nr}(S_1)/10^7$ s^{-1}		9.22			36.77	

[a] $\phi(S_1)$ of HgP^{4-} was determined by using H_2P^{4-} as reference,[19] $\Phi(S_1-B) = \phi(IC\ S_2 \rightarrow S_1) \times \phi(S_1)$ and $k_r(S_1) = \phi(S_1)/\tau(S_1)$.

S_1-fluorescence in its porphyrin complexes. These observations indicate that the schemes generally used in the porphyrin photophysics may need refinement: in the widely used Gouterman categorization of metalloporphyrins[154] only the electronic factor is taken into account, and the geometrical factor is also missing from Harriman's characterization for photophysical properties.[153,157]

Another kind of spin-allowed luminescence, that is, the rare S_2-fluorescence, is characteristic to porphyrins,[158] especially to monoporphyrins.[43] We found that, although HgP^{4-} also has an emission in this range, its concentration is so small that this very weak emission proved not to be reliably detectable.

The photophysical processes generally involve the triplet state(s) of molecules. One of the manifestations of the role of triplet activity is phosphorescence, whose lifetime and spectrum carries information about the properties of triplet-state molecules. Further information can be gained from triplet−triplet absorption. No phosphorescence of Hg^{II}-porphyrin complexes was observed at room temperature, so the only way of studying the properties of the triplet excited complexes is the observation of transient absorption. For the triplet-state porphyrins the maximum molar extinction coefficient is about a half of that of the corresponding ground state.[159] In our transient absorption experiments the concentration of the T_1-state was calculated from the bleaching of ground-state absorption, preferably at the wavelength of the bleaching maximum, which in our case coincides with the absorption maximum of the ground state. In the case of HgP^{4-}, because of the very low concentration, the transient absorption signal was so weak that only the triplet lifetime could be determined (Table 4). The individual transient signal of $Hg_2P_2^{8-}$ was not detectable because of the permanent presence of monomer or $Hg_3P_2^{6-}$. The spectra of the latter were also noisy, even when it was the dominant complex in the solution.

Only the $T_1 \rightarrow T_3$ transitions can be measured with our equipment. Using this absorption, the triplet lifetime of the free-base ligand was found to be 487 μs, in good agreement with the literature data of 400,[160] 420,[87] 459 ± 16,[161] and 414 μs.[162] For HgP^{4-}, $\tau(T_1) = 307$ μs was obtained, and for the solution of $Hg_3P_2^{6-}$, $\tau(T_1) = 7$ μs. There are two triplet lifetime determinations available in the literature for mercury(II) TPP: 320[78] and 32 μs.[151] The former value may refer to the 1:1 complex, but the latter might have been determined for a solution containing a mixture of complexes, mostly the 3:2 species. We think that the wider selection of vibrational modes

TABLE 4: The T_1 Transient Absorption Data of Free-Base and Mercury(II) Porphyrins[a]

species	H_2P^{4-}	HgP^{4-}	$(Hg_3P_2^{6-})^b$
$\tau(T_1)/\mu$s	487	307	7
$k_q(O_2)/10^9$ M^{-1} s^{-1}	1.59	2.40	2.23
$\Delta\epsilon(T_1)_{max}/10^5$ M^{-1} cm^{-1}	0.87		2.15
λ ($\Delta\varepsilon$)/nm	436		424
$\varepsilon(T_1)_{max}/10^5$ M^{-1} cm^{-1}	1.74		5.42
λ (ε)/nm	420		426
$E(T_3\text{-}S_2)$ ($\Delta\varepsilon$)/cm^{-1}	−1227		513
$E(T_3\text{-}S_2)$ (ϵ) /cm^{-1}	−353		402

[a] $\Delta\varepsilon(T_1)$ is the molar difference transient absorbance, addition of which to the ground-state absorbance resulted in the individual $\varepsilon(T_1)$ data. [b] Data for the solution in which the dominant species is the $Hg_3P_2^{6-}$complex, but the signal probably originates from a photoproduct (see text for details).

in the more complicated structure causes the significant decrease of lifetime. The heavy-atom effect of the out-of-plane metal center is probably not the dominant factor, similarly to the complexes of Ga^{3+}, In^{3+}, Tl^{3+}, Sn^{2+}, and Pb^{2+} ions whose lifetime is essentially independent of the metal centers.[163] Furthermore, very similar transient absorption spectra can be observed for other out-of-plane complexes, indicating that their triplet structures are considerably alike. This structure is probably more distorted than that of the ground state, based on enhanced red shift and on semiempirical quantum chemical calculations.[164] The published molar triplet extinction coefficients and absorption maxima for the free-base ligand (or H_2TPP) show significant scatter: ε_T(450 nm) = 25 150 M^{-1} cm^{-1} (calculated from maximum bleaching: 1.04×10^5 M^{-1} cm^{-1}),[160] ε_T(460 nm) = 1.30×10^5 M^{-1} cm^{-1} [87] and ε_T(440 nm) = 4.40×10^4 M^{-1} cm^{-1}.[165] The value we determined for ε_{Tmax} of the free-base porphyrin (1.74×10^5 M^{-1} cm^{-1}) is slightly higher than those in the literature but still in accordance with them. As to the rate constant for the quenching by O_2, our value ($k_q(O_2) = 1.59 \times 10^9$ $M^{-1}s^{-1}$) is in a good agreement with that reported earlier (1.82 ± 0.07) $\times 10^9$ M^{-1} s^{-1}.[161] For mercury(II) porphyrins neither the molar triplet absorbance, nor the O_2 quenching constants (Table 4) have been published so far. The quenching rate constants for these complexes are only slightly higher than that of the free-base ligand, indicating that the metal center hardly influences the oxygen sensitivity of the ligand-centered triplet excited state.

The ground-to-second singlet energy gap is generally larger than the corresponding triplet gap between T_3 and T_1. By subtracting the energy of $S_0 \rightarrow S_2$ absorption from that of $T_1 \rightarrow T_3$,

SCHEME 1: Photoinduced Reactions of $Hg_3P_2^{6-}$ with Their Quantum Yield at Soret-Excitation

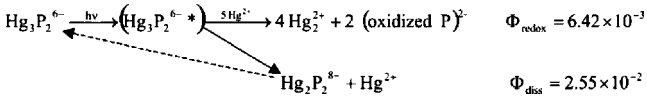

TABLE 5: The Photochemical Quantum Yields of the Free-Base and Mercury(II) Porphyrins in Air Saturated and Deoxygenated Solution[a]

species	H_2P^{4-}	HgP^{4-}	$Hg_2P_2^{8-}$	$Hg_3P_2^{6-}$
$\Phi(B)/10^{-5}$	0.60	22.4	15.8	3193
% dissociation		23%	20%	80%
$\Phi(B-Ar)/10^{-5}$	0.33	22.3	16.6	2969
% dissociation		13%	30%	77%
$\Phi(Q)/10^{-5}$		26.6	3.08	133
% dissociation			54%	80%
$\Phi(Q\text{-}Ar)/10^{-5}$		32.9	4.91	206
% dissociation			42%	88%

[a] $\Phi(B)$ and $\Phi(Q)$ are the overall photochemical quantum yields observed in Soret- and Q-band photolysis, and "% dissociation" denotes the photodissociation fraction of the overall quantum yield.

we obtain a positive number for the solution containing mostly the 3:2 complex. This is the opposite to the general observation and is an additional indication that the absorbing species is not the 3:2 complex in T_1 state. Hence, the measured absorption signal presumably originated from $Hg_2P_2^{8-}$, a product of the efficient photoinduced dissociation of the 3:2 complex (see below).

Primary Photochemistry. The porphyrins are efficiently applied in photosensitizations[78] and artificial photosynthesis;[151] however, very little is known about the role of the metal center in the photochemical processes if it is located out of the porphyrin plane, except that such complexes were reported to be photochemically labile.[166] In regard of the Hg^{II}-porphyrin complexes, no data concerning the primary photochemistry of the most studied OOP complex, $Hg_3P_2^{6-}$ have been reported in the literature, and nothing is available about the photoinduced reactions of the 1:1 and 2:2 complexes. In our earlier investigation of the primary photochemical reactions,[16,43] the importance of electron ejection was found to be unimportant. The two primary light-induced photochemical processes that metalloporphyrins were observed to undergo are photooxidation and photodecomposition, as is sketched for $Hg_3P_2^{6-}$ in Scheme 1.

The quantum yields of the photochemical processes in the form of the overall yield for the disappearance of the metalloporphyrin excited and its fraction that leads to photodissociation are listed in Table 5. One can see that the photoreactivity is increased by orders of magnitude due to coordination of one Hg^{2+} ion to the porphyrin, dimerization of HgP^{4-} somewhat reduces it, and formation of the 3:2 complex significantly enhances it. The quantum yields depend on the energy of the excitation. The free-base porphyrin does not suffer measurable chemical change if excited at the Q-band. The yield of the overall photoreaction of the 1:1 complex is essentially the same irrespective of the excitation band; the yield in the bisporphyrins is much higher when they absorb at the Soret band than at the Q-band. While HgP^{4-} does not photodissociate upon longer-wavelength excitation, the bisporphyrins do, and the relative importance of photodissociation is essentially wavelength-independent. The 3:2 complex exhibits especially large photoactivity. Compared with $Hg_2P_2^{8-}$ the photochemical quantum yield increases by about 2 orders of magnitude. The reason can be found in the structure of the complex (see later): between three Hg ions two porphyrin rings are sandwiched. The outer mercury(II) ions are much farther out of the porphyrin ring than in the 2:2 complex, so that either of them can be easily ejected upon excitation, especially following a ligand-to-metal charge transfer (LMCT). This phenomenon confirms that for the increased efficiency of the photoredox process in these metalloporphyrins (compared to that in the case of free-base porphyrin), the position and not the redox potential of the metal center is responsible, in accordance with the discussion below.

According to the literature, in the photolysis of in-plane complexes no photooxidation of the macrocycle can be observed, for example, for palladium(II)[87] and aluminum(III) porphyrins.[167] In the case of some out-of-plane metalloporphyrins, for example, tin(II)[168] and (di)thallium(I),[169] or borderline cases,[8,43] for example, magnesium(II)[167,170] and zinc(II),[168−170] photooxidation does occur. In this reaction, the metal ion is temporarily reduced and the ligand is oxidized. The latter suffers ring-opening and eventually forms open-chain dioxo-tetrapyrrol derivatives, bilindions[169,171−173] (note that in living organisms enzymatic processes alter the decomposition pathway).[174] The reduced metal ion is released when the macrocycle breaks, transfers its electron to other particles in the solution, and gets back to its stable oxidized form. Hg^{2+} ions are in this respect exceptional, as the reduced form, Hg_2^{2+} is also stable. We confirmed the formation of the reduced form of the metal ion by spectrophotometrically[156,175] detecting the Hg_2^{2+} ions formed in the photooxidation of $Hg_3P_2^{6-}$ which supports the proposed mechanism.

The photoinduced ring-oxidation can also be observed for the free-base ligand, although with very low quantum yield.[15−20,176] Metalation increases this quantum yield, which can be rationalized by assuming that an irreversible, probably indirect photoinduced LMCT takes place. The enhancement of the rate of photooxidation is more expressed if the chance of backward metal-to-ligand charge transfer (MLCT) is drastically decreased which is the case in out-of-plane complexes where the metal ion is far from the porphyrin cavity. As mentioned above, the possibility of electron ejection can essentially be excluded, so that the only process is LMCT that can cause the metal-induced increase of the photooxidation quantum yield.

In principle, the photooxidation could take place due to the oxygen present in the solution. To reveal the role of O_2, we measured the quantum yield of the photochemical loss of all three mercury-porphyrins as well as the bare ligand in air saturated as well as in deoxygenated, that is, argon-saturated solution. The quantum yields for the overall loss of our metalloporphyrins, including both the photooxidation and the photodissociation, listed in Table 5 are within 7% identical in the presence or absence of O_2 if measured at the Soret band, but 25−55% larger in the absence of O_2 if determined at the Q-band. This means that the dissolved oxygen does not participate in the photooxidation. The increase of the yield obtained at the Q-band if oxygen is absent suggests that the indirect LMCT process probably originates from some tiplet state, which can be quenched by oxygen. No such quenching can be observed if the excitation is at the Soret band, indicating that the higher excited triplet state has a much smaller role in the photochemistry. A series of observations listed below reveals a significant difference between the photochemical activity of the lower and higher excited states. Namely, in HgP^{4-} only the first excited states are photochemically reactive: the photooxidation quantum yield at Soret-excitation is almost equal to the product of the quantum yield at Q-excitation (Table 5) and the efficiency of the $S_2 \rightarrow S_1$ internal conversion (about 70%, see

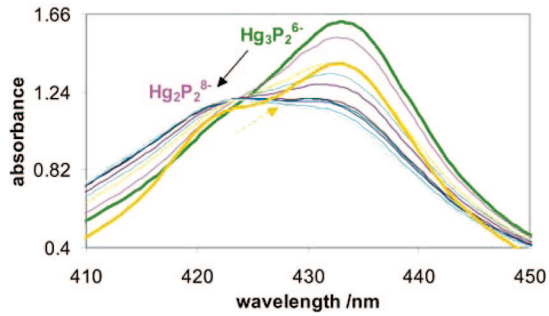

Figure 8. The absorption spectra taken in 1 s intervals during the photolysis ($I = 1.07 \times 10^{-5}$ M photon/s at $\lambda_{irr} = 433$ nm) of a solution containing 6.9×10^{-6} M porphyrin and 1.5×10^{-3} M mercury(II) ion (measured in a 1 cm cuvette). The thick green line represents the spectrum before the photolysis, and the orange line represents the spectrum measured one hour after the irradiation was stopped.

Table 3). In contrast, the second excited states of bisporphyrins are significantly more reactive than the first ones. Furthermore, the planar (free-base and in-plane metallo-) porphyrins decompose only in the photolysis at the Soret-band, and Q-excitation is not sufficient either for the photodissociation of OOP monoporphyrins,[15,18,19,43] for example, HgP^{4-} (Table 5).

There are some indications that an intersystem crossing process takes place starting from the S_2 state. One of these is that the photooxidation of H_2P^{4-} and of $Hg_3P_2^{6-}$ is quenched by O_2. Such ISCs can occur as a consequence of the rigidity of a macrocycle.[177] The unquenchable fraction in argon-saturated solution of free-base ligand can cause CTTS (charge transfer to solvent) from the S_2-state, but its efficiency does not increase significantly owing to metalation.[16,43]

Now we turn to the results related to the photodissociation of Hg^{II}-porphyrin complexes. These processes take place mainly in polar solvents.[15−20,43] Under these conditions the absorption bands of the fragments of the original metalloporphyrin appear during photolysis. The process is reversible; thus, if the irradiation is discontinued the initial complex recovers within a certain time (Figure 8.). The dissociation product of HgP^{4-} is the free-base ligand, similarly to other metallo-monoporphyrins.[15,18,19,43] Free-base porphyrin can also be formed in the photodissociation of bisporphyrins. If $Hg_2P_2^{8-}$ is photolyzed, the quantum yield of the formation of free-base porphyrin is small, the major product being the monomer. The photodissociation of $Hg_3P_2^{6-}$ results purely in the formation of the 2:2 complex (Scheme 1 and Figure 8). An additional difference between the mono- and bisporphyrins is that the repulsive potential surface corresponding to dissociation can cross that of also the first excited states of the latter species, while, for the previous complexes dissocation can be originated only from the second excited states populated by Soret-band irradiation.

DFT Calculations. The main purpose of our electronic structure calculations is to reveal the geometrical structure of the 1:1, 2:2, and 3:2 complexes of Hg^{2+} with porphyrin and to detect whether there is a correlation between the features of geometry and the electronic spectrum. In the calculations, we used a model in which the sulfonato-phenyl substituents of the porphyrin ligand, present in our experiments, were omitted. We expect that the out-of-plane distortion of the ligand, influenced mainly by the interaction and relative size of the cavity and the metal ion, can be correctly described with this model. Exploratory calculations with the tetraphenyl-porphyrin ligand indicate that the structure and spectra of HgTPP do not significantly differ from those of HgP.

The insertion of the Hg^{2+} ion into the porphyrin causes a significant distortion of the macrocycle. According to the commonly used reasoning, the relative size of the metal ion as compared to the cavity of the ligand determines the magnitude of distortion. Listed in Table 6 are the calculated geometrical parameters related to the size of the cavity and the geometrical distortion of the macrocycle obtained for the ligand and the 1:1, 2:2, and 3:2 mercury(II)-porphyrin. The parameters presented are d(N−N), the distance between diagonally located N atoms, which is a measure of distortion of the cavity size; d_{OOP}, the distance between the metal atom and the plane of the four N atoms, which is a measure of the magnitude of protrusion of the Hg atom from the ligand; and d_{dome}, domedness, which we define as the distance between the plane of the four N atoms and that of the β carbon atoms, which characterizes the magnitude of the distortion of the macrocycle. This last measure of distortion is closely related to the doming angle proposed by Ricciardi et al.[40] for the same purpose.

Both the B3LYP/LANL2DZ and M05/LANL2DZ calculations reproduce the D_{2h} structure as the most stable structure of free-base porphyrin (Table 6). For the deprotonated species (P^{2-}), we obtain D_{4h} symmetry, in agreement with the expectation. The 4-fold symmetry is inherited by the monomer units of the metalloporphyrins we studied. As expected, in Hg^{2+}-porphyrin complexes the metal ion protrudes from the plane of the ligand the magnitude of which depends on the composition. The appealing explanation for this is that the diameter of Hg^{2+} (204 pm) is too large to fit coplanar into the cavity of the porphyrin ring. In the 1:1 complex, the distance of Hg^{2+} from the N atoms is 224 pm, which the bond length in a planar arrangement would push apart the N atoms to almost 450 pm from the 420 pm characterizing the deprotonated porphyrin. The high strain is released by lifting the Hg ion out of the plane of the N atoms so that the diagonal N−N separation can be as small as 436 pm. At the same time, the Hg and the four N atoms form a pyramid, which induces the distortion of the plane of the C_α carbon tier and through it the rest of the macrocycle.

We obtained a well-defined structure for the 3:2 complex, shown in Figure 9. In this structure two porphyrin rings sandwich one Hg ion, and there are two Hg ions coordinated to the outer side of both porphyrins. The three Hg ions are located along the same straight line which is also a C_2 symmetry axis of the complex. Because of the coordination on both sides, the ligand is almost planar (the domedness is less than 10 pm). The two porphyrin rings are rotated by 45° with respect to each other around the axis formed by the Hg ions so that the overall symmetry of the complex is D_{4d}. The outer Hg ions protrude almost twice as much as in the 1:1 complex, which suggests that they are sensitive to perturbation and can leave relatively easily. This is in agreement with the observed photolability of the 3:2 complex.

The Mayer bond orders[178−180] calculated for the bonds between the outer Hg ion and the N atoms of the neighboring porphyrin unit are 0.38, those between the inner Hg ion and the 8 N atoms are 0.12 each. Comparing with the Hg−N bond orders in the monomer, 0.35, one can see that the central Hg ion is coordinated to both prophyrin units and can be expected to couple the electronic states of the two monomers. As we have shown in the previous sections, there are well-defined experimental signs for this role both in the spectra and the photochemistry of the 3:2 complex.

The structure of the 2:2 complex is much more poorly defined. This constitution corresponds to two 1:1 complexes which proved to be bound together by relatively weak intermolecular forces. As the 1:1 monomers are not planar, several relative arrangements can be assumed. Two symmetric configurations

TABLE 6: The Calculated Structural Data of Unsubstituted Free-Base, Deprotonated, 1:1 and 3:2 Mercury(II) Porphyrins

species	H_2P		P^{2-}		HgP		$Hg_3P_2^{2+}$	
method	B3LYP	M05	B3LYP	M05	B3LYP	M05	B3LYP	M05
symmetry	D_{2h}	D_{2h}	D_{4h}	D_{4h}	C_{4h}	C_{4h}	D_{4h}	D_{4h}
d(N−N)/pm	407 (425)	406 (424)	420	418	436	435	413	412
d(Hg−N)/pm	102[a]	102[a]			224	225	241 (275[b])	241 (274[b])
d_{OOP}/pm					52	55	125 (182[b])	125 (181[b])
d_{dome}/pm					38	46	9	4
d(P−P)/pm							378	366

[a] d(H−N). [b] The data of the inner mercury(II) ion.

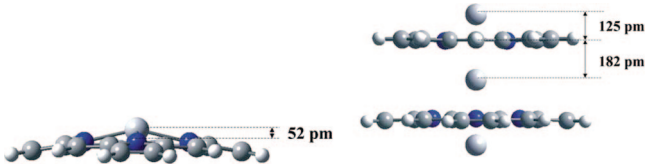

Figure 9. Structure of the 1:1 and 3:2 complex calculated at the B3LYP/LANL2DZ level.[18]

could be expected to be the most stable. In one of them, a face-to-face arrangement, the two ligands point toward each other and both metal ions point outside (like a pair of cymbals) and in the other, a P−Hg−P−Hg arrangement in which the Hg ion of one monomer points toward the cavity of the other (like two saucers, one placed into the other). In both structures the porphyrin rings can be eclipsed or be rotated by 45°. The rotated arrangements are truncated versions of the structure of the 3:2 complex (obtained formally by removing either the central or one of the outer Hg ions). Finding the corresponding minima of the potential surface proved to be extremely difficult with the B3LYP functional. For example, the binding energy of the dimer structures is found to be positive except for one, unusually distorted structure. Note that the basis set superposition error is not responsible for the inaccurate binding energy (it causes the opposite effect). Actually, the counterpoise correction was found to be much smaller than the energy difference to be corrected, probably because at the B3LYP/LANL2DZ level the two fragments are as far as 420 pm from each other. The poor performance of the B3LYP functional seems to be due to the inaccurate description of long-range interactions between the porphyrin π systems. In the following, we discuss only the structures obtained with the M05 functional.

Out of the four possible symmetric structures with C_{4v} symmetry, the eclipsed saucerlike (I) and the staggered cymballike (II) structures (Figure 10a,b) were found to be genuine minima (no negative eigenvalues of the Hessian) with binding energies of 26 and 11 kJmol^{-1}, respectively. The staggered saucerlike structure III (Figure 10c), although deeper in energy (32 kJmol^{-1}), is a second-order saddle point on the potential surface with motion corresponding to tilting the two macrocyles leading to energy reduction. The deepest-energy stucture we found is a Hg−P−Hg−P arrangement IV (Figure 10d, with C_s symmetry) in which one of the 1:1 monomers is shifted with respect to the other along the line passing two diagonally located N atoms by about 100 pm and is bound by about 36 kJmol^{-1}. The analogous cymballike (Hg−P−P−Hg) structure V (Figure 10e, C_{2h}) is less stable (its binding energy is 26 kJmol^{-1}) in which the two macrocycles are shifted by 359 pm. This structure is very similar to what we found for two stacked (planar) free-base porphyrin molecules. Several other minima were also found with remarkable binding energy, among them one (VI, Figure 10f) in which the porphyrin "planes" are at an angle of about 45° with respect to each other.

In these structures the geometry of the monomer units is essentially the same as in the free 1:1 complex. The Hg−N bond order is between 0.33 and 0.35. In the symmetric saucerlike dimers I and III, the inner Hg ion has a bond order of 0.33 to its "own" N atoms, and its bond to the N atoms of the other porphyrin ring is characterized by a bond order of 0.01 or 0.02. This indicates that, in contrast to the 3:2 complex, the Hg ion has a minor role in binding together the two porphyrin units of the 2:2 complex. One can see, however, that this role is not negligible; the saucerlike structures are more strongly bound and the Hg−N bond orders are not zero. In the cymballike and the shifted arrangements, the intermonomer Hg−N bond order is negligible (<0.001). The dominant interaction holding together the monomers is probably the $\pi-\pi$ interaction. The interplay of the two effects determines the distance between the monomers. In the cymballike C_{4v} structure d(P−P) $\approx$ 420 pm. It is remarkable, however, that the "planes" of the monomers get much closer if they are shifted with respect to each other (structure V, d(P−P) $\approx$ 355 pm) in agreement with the significant increase of the binding energy, indicating the efficiency of the $\pi-\pi$ interaction. In the saucerlike structures, d(P−P) tends to be smaller than in the symmetric cymballike dimer; in the C_{4v} species (I, III, and in IV), it is about 385 pm (cf. 366 pm in the 3:2 complex). This distance is close to but somewhat larger than in the lanthanide(III) bis- or trisporphyrins (where d(P−P) is around 260−350 pm depending on radius of metal ion[37]). In the latter sandwich complexes,[40,143] as well as in the most studied bisporphyrins, oxodimers,[33,181] the two ligands are staggered, while the Hg^{II} porphyrins seem to be more flexible in this respect.

The solvent, in principle, can further stabilize the complexes, for example, by bridging the two fragments. We attempted to estimate the possible bridge-formation by water molecules (as the experiments were done in aequous solution) but no stable configuration was found. We think that the 2:2 complex has numerous stable relative arrangements, but there is no information on how easily they are interconverted. On the basis of the experimental observation that the 2:2 complex is easily formed from the 3:2 one, one can expect that the saucerlike Hg−P−Hg−P geometry is primarily generated when the 3:2 complex decomposes by splitting off one of the terminal Hg ions.

The macrocycle distortion from the planar structure is characterized by d_{dome} values of about 40 pm in the monomer and both types of the dimer. In our calculations on other typical 1:1 out-of-plane complexes, we obtained very similar domedness.[43] As the spectral, photophysical, and photochemical properties of several OOP porphyrins are very similar, it would be reasonable to assume that the common property, the doming, is the source of the common properties. More information can be drawn from the observation that in the 3:2 complex the distortion is significantly reduced with respect to the 1:1 or 2:2 complexes because both porphyrin rings are embedded between two metal centers (Figure 9). Two metal centers located

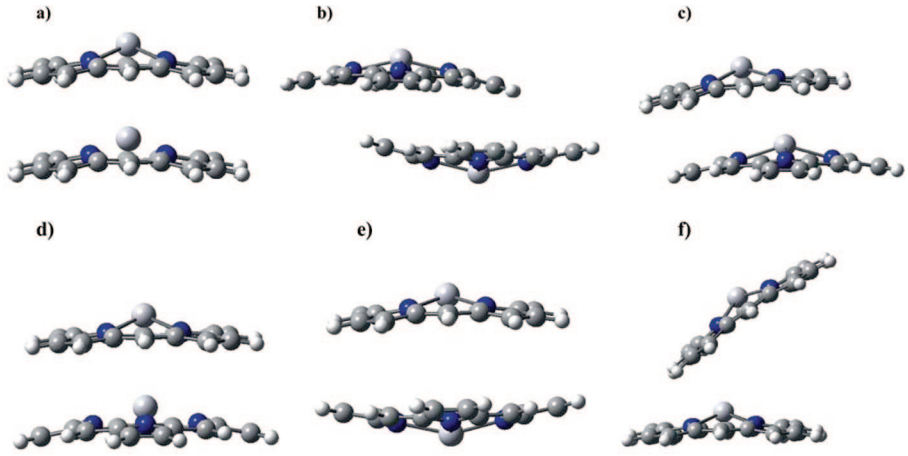

Figure 10. The structure of 6 metastable isomers of Hg_2P_2 dimer obtained at the M05/LANL2DZ level of theory.

TABLE 7: Structural Data of Isomers of Hg_2P_2 Dimer Obtained at the M05/LANL2DZ Level of Theory (Figure 10)

isomer	a	b	c	d	e	f
symmetry	C_{4v}	C_{2h}	C_1	C_{4v}	D_{4d}	C_1
d(N−N)/pm	431	436	433	429	435	434
	433		433	432		432
d(Hg−N)/pm	227	224	225	226	224	225
	227[b]		226[b]	226[b]		226[b]
	316[b]			375[b]		
d_{OOP}/pm	70			69		
	68[b]	52	63	71[b]	52	57
	316[b]		67[b]	308[b]		66[b]
d_{dome}/pm	48	50	44	35	46	44
	53		45	44		44
d(P−P)/pm	387	364	372	382	420	426
ΔE/kJ mol^{-1}[a]	−26.3	−31.8	−35.8	−32.1	−11.3	−23.5

[a] Dimerization energy. [b] The data of the inner mercury(II) ion.

TABLE 8: The Absorption Data According to M05 Calculations for Unsubstituted Deprotonated, Free-Base, Dimer of Free-Base, 1:1 and 3:2 Mercury(II) Porphyrins[a]

species	P^{2-}	H_2P		$(H_2P)_2(C_i)$		HgP	$Hg_3P_2^{2+}$
transition symmetry	E_u	$y = B_{2u}$	$x = B_{1u}$	$y = A_u$	$x = A_u$	E	E_2
λ(B)/nm	357	347	367	337	364	359	331
f(B)	1.40	0.95	0.47	1.13	0.71	1.72	1.25
B-shift/cm^{-1}	3			559		−200	2191
λ(Q)/nm	701	509	550	518	555	528	537
f(Q)	0.0204	0.0005	0.0022	0.0034	0.0065	0.0022	0.0365
Q-shift/cm^{-1}	−4643			−254		33	−274

[a] The wavelengths and shifts were calculated from the average of y and x transitions; f is the oscillator strength.

symmetrically on both sides of a single porphyrin ring can actually restore the planarity of the macrocycle which actually is observed in our electronic structure calculations on the 2:1 complex of Tl^+ or Hg_2^{2+} and porphyrin.[18,43]

The significant difference between the magnitude of doming of the 1:1 and 3:2 complexes suggests that, as long as the distortion of the macrocycle is a dominant factor among those determining the spectral characteristics, then one can expect a significant difference between the spectra of the two complexes. In addition, the 2:2 complex should in this respect resemble more the monomer than the 3:2 complex, as the doming is essentially the same in the 1:1 and 2:2 complexes. A factor that may be important in refining this picture is that in the bisporphyrins the two macrocycles are located close to each other so that their π-electron systems can interact and the $\pi-\pi$ interaction can influence the ground and excited states differently. What we observed experimentally is that the Soret-band of the dimer is very similar to that of the monomer (apart from the broadening), and the Q-bands resemble those of the 3:2 complexes (Figures 5 and 6).

To understand the role of the macrocycle distortion, we calculated electronic spectra using the TD-DFT method (Tables 8 and 9). The basic principles for the assignment of the transitions were laid down in Gouterman's 4 MO model.[46] The transitions in the monomers take place between the frontier orbitals. The Soret- and the Q-bands, according to our calculations (in agreement with the literature, see for example refs 40 and 182) were not found to be pure one-electron excitations but mixtures of them, often with several one-electron excitations superposed with comparable weight; in other words, configuration interaction is essential here. The transitions from the nearly degenerate HOMO-1 + HOMO to the truly degenerate LUMO in an idealized D_{4h} symmetrical structure go from $a_{1u} + a_{2u}$ to e_g, and the corresponding absorption bands should split with the decrease of symmetry, more precisely, the disappearance of 4-fold rotation axis. The TD-DFT calculations do show

TABLE 9: The Absorption Data of Isomers of Hg_2P_2 Dimer (Fig. 10) from M05/LANL2DZ Calculations

isomer	a	b	c	d	e	f
transition-symmetry	E	A	A	E	E_2	A
λ(B)/nm	346	360	349	349	348	353
f(B)	2.00	1.89	1.58	1.84	2.12	2.50
B-shift/cm^{-1}	915	−277	653	630	689	261
λ(Q)/nm	528	531	532	533	533	536
f(Q)	0.0014	0.0022	0.0024	0.0036	0.0032	0.003
Q-shift/cm^{-1}	38	−89	−111	−152	−160	−259

such a splitting but experimentally it is not visible in the region of the Soret band. This discrepancy may be one of the reasons why the calculated Soret-band positions are farther from the experiments than those of the Q-band. The experimental observation is that both absorptions shift to the red region of spectra in the series of free-base ligand, 1:1, 2:2, and 3:2 complexes (Tables 1 and 2). The TD-DFT calculations (Tables 8 and 9) show the same tendency for the Q-band of 1:1, 2:2, and 3:2 complexes, but not for the Soret band. The highest red shift of this band was calculated for the deprotonated porphyrin, which can be interpreted as follows: in the deprotonated porphyrin all four pyrrol-nitrogens can take the same proportion in the delocalization, while the diagonally placed pairs of pyrrols are different in the free-base (twice protonated) porphyrin. The deprotonation causes the increase of aromatization, resulting in the bathochrom effect of the spectrum. This suggests that in an out-of-plane complex the electronic properties of macrocycle approach that of P^{2-}. The spectra become more complicated on going from mono- to bisporphyrins. What we can see is the two chromophores are not fully uncoupled (their molecular orbitals are mixed), and the transitions have even less one-electron excitation nature than in the monomers.

Several earlier studies concerned the role of the porphyrin distortion in determining the characteristics of electronic spectra of metalloporphyrins. Shelnutt and co-workers[1,183,184] showed that the red shift of the $\pi\pi^*$ absorption bands is very a sensitive probe of the saddle and ruffle distortion of the macrocyle. They found that the correlation is not linear and not one-to-one, as there are numerous other factors that influence the energy levels of metalloporphyrins. Similar conclusions can be seen from the work of Ricciardi et al.[40] for some dome-distorted porphyrins. On the basis of our results, we think that the dome distortion is not the only factor responsible for the common behavior of out-of-plane porphyrins.

Conclusions

Mercury(II) porphyrins as the model compounds of out-of-plane metalloporhyrins were extensively characterized from the viewpoints of composition, equilibria, kinetics of formation, and spectroscopic properties as well as photophysics, photochemistry, and quantum chemistry. These features were carefully investigated with the purpose of elucidating the effects of the metal center in an out-of-plane position. Mercury(II) ion can form not only 1:1 but bisporphyrin complexes also, and the 2:2 species was identified for the first time in this work, significantly promoting the confirmation of the composition and the precise elucidation of the equilibrium of $Hg_3P_2^{6-}$. The insertion of Hg^{2+} into the cavity of the ligand is one of the fastest among the metalation reactions of porphyrins, and the formed 1:1 complex dimerizes very fast. The photoinduced properties of the bisporphyrins are quite different from those of HgP^{4-}. Their absorption bands are broader, their fluorescence is not detectable, the lifetime of their triplet excited states is shorter, and they are photochemically more reactive. The trimercury(II) bisporphyrin has a unique photochemical activity among metalloporphyrins; it displays the highest efficiencies for both photoredox reaction and photodissocation. The electronic structure calculations confirm that in the 1:1 and 2:2 complex the Hg ion is located out of the porphyrin plane, and at the same time the macrocycle is dome-distorted in the opposite direction. The calculations using the M05 functional indicate the existence of several possible isomers of the 2:2 complex which is a loosely bound dimer of 1:1 units, the most stable being a reduced-symmetry species. The energy levels of the complexes, as well as the overall characteristics of the spectral properties are reproduced by TD-DFT calculations, but the magnitude of the line shifts are not. The calculations indicate that the change of the spectral characteristics cannot be assigned solely to the distortion of the porphyrin ring.

Further studies for the characterization of other typical OOP metalloporphyrins in respects of structural, kinetic, and photo-induced features are in progress in our laboratory in order to establish general tendencies in the properties of this type of complexes.

Acknowledgment. Support of this work by the Hungarian Scientific Research Fund (OTKA O.H.: K63494, G.L.: T049257) is gratefully acknowledged.

References and Notes

(1) Shelnutt, J. A.; Song, X.-Z.; Ma, J.-G.; Jia, S.-L.; Jentzen, W.; Medforth, C. J. *Chem. Soc. Rev.* **1998**, *27*, 31.
(2) Song, X.-Z.; Jaquinod, L.; Jentzen, W.; Nurco, D. J.; Jia, S.-L.; Khoury, R. G.; Ma, J.-G.; Medforth, C. J.; Smith, K. M.; Shelnutt, J. A. *Inorg. Chem.* **1998**, *37*, 2009.
(3) Fischer, M. S.; Weiss, C. *J. Chem. Phys.* **1970**, *53*, 3121.
(4) Barkigia, K. M.; Berber, M. D.; Fajer, J.; Medforth, C. J.; Renner, M. W.; Smith, K. M. *J. Am. Chem. Soc.* **1990**, *112*, 8851.
(5) Hoard, J. L. *Science* **1971**, *174*, 1295.
(6) Stanley, K. D.; Luo, L.; de la Vega, R. L.; Quirke, J. M. E. *Inorg. Chem.* **1993**, *32*, 1233.
(7) Kozlowski, P. M.; Rush, T. S.; Jarzecki, A. A.; Zgierski, M. Z.; Chase, B.; Piffat, C.; Ye, B.-H.; Li, X.-Y.; Pulay, P.; Spiro, T. G. *J. Phys. Chem. A* **1999**, *103*, 1357.
(8) Barnes, J.; Dorough, G. *J. Am. Chem. Soc.* **1950**, *72*, 4045.
(9) Fleischer, E. B.; Wang, J. H. *J. Am. Chem. Soc.* **1960**, *82*, 3498.
(10) Treibs, A. *Liebigs Ann. Chem.* **1969**, *728*, 115.
(11) Abraham, R. J.; Hawkes, G. E.; Hudson, M. F.; Smith, K. M. *J. Chem. Soc., Perkin Trans. 2* **1975**, 205.
(12) Hove, E.; Horrocks, W. D. *J. Am. Chem. Soc.* **1978**, *100*, 4386.
(13) Barkigia, K. M.; Fajer, J.; Adler, A. D.; Williams, G. J. B. *Inorg. Chem.* **1980**, *19*, 2057.
(14) Callot, H. J.; Chevrier, B.; Weiss, R. *J. Am. Chem. Soc.* **1979**, *101*, 7729.
(15) Horváth, O.; Valicsek, Z.; Vogler, A. *Inorg. Chem. Commun.* **2004**, *7*, 854.
(16) Valicsek, Z.; Horváth, O.; Stevenson, K. L. *Photochem. Photobiol. Sci.* **2004**, *3*, 669.
(17) Huszánk, R.; Horváth, O. *J. Chem. Soc., Chem. Commun.* **2005**, 224.
(18) Horváth, O.; Huszánk, R.; Valicsek, Z.; Lendvay, G. *Coord. Chem. Rev.* **2006**, *250*, 1792.
(19) Valicsek, Z.; Horváth, O. *J. Photochem. Photobiol. A.* **2007**, *186*, 1.
(20) Huszánk, R.; Lendvay, G.; Horváth, O. *J. Biol. Inorg. Chem.* **2007**, *12*, 681.

(21) Grant, C.; Hambright, P. *J. Am. Chem. Soc.* **1969**, *91*, 4195.
(22) Hambright, P. *Coord. Chem. Rev.* **1971**, *6*, 247.
(23) Shamim, A.; Hambright, P. *J. Inorg. Nucl. Chem.* **1980**, *42*, 1645.
(24) Robinson, L. R.; Hambright, P. *Inorg. Chem.* **1992**, *31*, 652.
(25) Tabata, M. *J. Mol. Liq.* **1995**, *65/66*, 221.
(26) Tabata, M.; Miyata, W.; Nahar, N. *Inorg. Chem.* **1995**, *34*, 6492.
(27) Haye, S. E.; Hambright, P. *Inorg. Chem.* **1984**, *23*, 4777.
(28) Vilaplana, R. A.; González-Vílchez, F. *J. Chem. Soc., Dalton Trans.* **1993**, 1779.
(29) Akins, D. L.; Zhu, H. R.; Guo, C. *J. Phys. Chem.* **1994**, *98*, 3612.
(30) Akins, D. L.; Zhu, H. R.; Guo, C. *J. Phys. Chem.* **1996**, *100*, 5420.
(31) Akins, D. L.; Özcelik, S.; Zhu, H. R.; Guo, C. *J. Phys. Chem.* **1996**, *100*, 14390.
(32) Chang, C. K. L. *Heterocycl. Chem.* **1977**, *14*, 1285.
(33) Lay, K. L.; W. Buchler, J.; Kenny, J. E.; Scheidt, R. *Inorg. Chim. Acta* **1986**, *123*, 91.
(34) Hofmann, J. A.; Bocian, D. F., Jr *J. Phys. Chem.* **1984**, *88*, 1172.
(35) Hudson, M. F.; Smith, K. M. *J. Chem. Soc. Chem. Commun.* **1973**, 515.
(36) Hudson, M. F.; Smith, K. M. *Tetrahedron Lett.* **1974**, *26*, 2223.
(37) Duchowski, J. K.; Bocian, D. F. *J. Am. Chem. Soc.* **1990**, *112*, 8807.
(38) Bilsel, O.; Rodriguez, J.; Milam, S. N.; Gorlin, P. A.; Girolami, G. S.; Suslick, K. S.; Holten, D. *J. Am. Chem. Soc.* **1992**, *114*, 6528.
(39) Wittmer, L. L.; Holten, D. *J. Phys. Chem.* **1996**, *100*, 860.
(40) Ricciardi, G.; Rosa, A.; Baerends, E. J.; van Gisbergen, S. A. J. *J. Am. Chem. Soc.* **2002**, *124*, 12319.
(41) Ledon, H. J.; Bonnet, M. *J. Am. Chem. Soc.* **1981**, *103*, 6209.
(42) Knör, G. *Coord. Chem. Rev.* **1998**, *171*, 61.
(43) Valicsek, Z.; Huszánk, R.; Lendvay, G.; Horváth, O. Unpublished work, 2008.
(44) Spanjaard, C.; Berthier, G. *J. Chim. Phys. Phys.-Chim. Biol.* **1961**, *58*, 169.
(45) Chantrell, S. J.; McAuliffe, C. A.; Munn, R. W.; Pratt, A. C. *Coord. Chem. Rev.* **1975**, *16*, 259.
(46) Gouterman M. *The Porphyrins*; Dolphin, D., Ed.; Academic Press: New York, 1978; Vol. III.
(47) Corwin, A. H. *J. Am. Chem. Soc.* **1963**, *85*, 3621.
(48) Biesaga, M.; Pyrzynska, K.; Trojanowicz, M. *Talanta* **2000**, *51*, 209.
(49) Delmarre, D.; Méallet, R.; Bied-Charreton, C.; Pansu, R. B. *J. Photochem. Photobiol., A.* **1999**, *124*, 23.
(50) Zhang, X. B.; Guo, C. C.; Li, Z. Z.; Shen, G. L.; Yu, R. Q. *Anal. Chem.* **2002**, *74*, 821.
(51) Cano-Raya, C.; Fernández-Ramos, M. D.; Gómez-Sánchez, J.; Capitán-Vallvey, L. F. *Sens. Actuators, B* **2006**, *117*, 135.
(52) Dolci, L. S.; Marzocchi, E.; Montalti, M.; Prodi, L.; Monti, D.; Di Natale, C.; D'Amico, A.; Paolesse, R. *Biosens. Bioelectron.* **2006**, *22*, 399.
(53) Kobayashi, N. *J. Porphyrins Phthalocyanines* **2000**, *4*, 377.
(54) Gentemann, S.; Medforth, C. J.; Ema, T.; Nelson, N. Y.; Smith, K. M.; Fajer, J.; Holten, D. *Chem. Phys. Lett.* **1995**, *245*, 441.
(55) Karger, G. A.; Reid, J. D.; Hunter, C. N. *Biochemistry.* **2001**, *40*, 9291.
(56) Sazanovich, I. V.; Berezin, D. B.; van Hoek, A.; Panarin, A. Y.; Bolotin, V. L.; Semeykin, A. S.; Chirvony, V. S. *J. Porphyrins Phthalocyanines* **2005**, *9*, 59.
(57) Drain, C. M.; Kirmaier, C.; Medforth, C. J.; Nurco, D. J.; Smith, K. M.; Holten, D. *J. Phys. Chem.* **1996**, *100*, 11984.
(58) Vitasovic, M.; Gouterman, M.; Linschitz, H. *J. Porphyrins Phthalocyanines* **2001**, *5*, 191.
(59) Nguyen, K. A.; Day, P. N.; Pachter, R. *J. Phys. Chem. A* **1999**, *103*, 9378.
(60) Kobayashi, N. *J. Porphyrins Phthalocyanines* **2000**, *4*, 377.
(61) Wertsching, A. K.; Koch, A. S.; DiMagno, S. G. *J. Am. Chem. Soc.* **2001**, *123*, 3932.
(62) Weinkauf, J. R.; Cooper, S. W.; Schweiger, A.; Wamser, C. C. *J. Phys. Chem. A* **2003**, *107*, 3486.
(63) Tsai, H.-H. G.; Simpson, M. C. *J. Phys. Chem. A* **2004**, *108*, 1224.
(64) Cramariuc, O.; Hukka, T. I.; Rantala, T. T. *J. Phys. Chem. A* **2004**, *108*, 9435.
(65) Ryeng, H.; Ghosh, A. *J. Am. Chem. Soc.* **2002**, *124*, 8099.
(66) Barkigia, K. M.; Chantranupong, L.; Smith, K. M.; Fajer, J. *J. Am. Chem. Soc.* **1988**, *110*, 7566.
(67) Fonda, H. N.; Gilbert, J. V.; Cormier, R. A.; Sprague, J. R.; Kamioka, K.; Connolly, J. S. *J. Phys. Chem.* **1993**, *97*, 7024.
(68) Nguyen, K. A.; Day, P. N.; Pachter, R.; Tretiak, S.; Chernyak, V.; Mukamel, S. *J. Phys. Chem. A* **2002**, *106*, 10285.
(69) Wasbotten, I. H.; Wondimagegn, T.; Ghosh, A. *J. Am. Chem. Soc.* **2002**, *124*, 8104.
(70) Haddad, R. E.; Gazeau, S.; Pécaut, J.; Marchon, J-C.; Medforth, C. J.; Shelnutt, J. A. *J. Am. Chem. Soc.* **2003**, *125*, 1253.
(71) Song, Y.; Haddad, R. E.; Jia, S.-L.; Hok, S.; Olmstead, M. M.; Nurco, D. J.; Schore, N. E.; Zhang, J.; Ma, J.-G.; Smith, K. M.; Gazeau, S.; Pécaut, J.; Marchon, J.-C.; Medforth, C. J.; Shelnutt, J. A. *J. Am. Chem. Soc.* **2005**, *127*, 1179.
(72) Mack, J.; Asano, Y.; Kobayashi, N.; Stillman, M. J. *J. Am. Chem. Soc.* **2005**, *127*, 17697.
(73) Mack, J.; Stillman, M. J.; Kobayashi, N. *Coord. Chem. Rev.* **2007**, *251*, 429.
(74) Fleischer, E. B.; Palmer, J. M.; Srivastava, T. S.; Chatterjee, A. *J. Am. Chem. Soc.* **1971**, *93*, 3162.
(75) Baker, H.; Hambright, P.; Ross, L. *Inorg. Chem.* **1973**, *12*, 2200.
(76) Harriman, A. *Coord. Chem. Rev.* **1979**, *28*, 147.
(77) Kalyanasundaram, K.; Grätzel, M. *Helv. Chim. Acta* **1980**, *63*, 478.
(78) Kalyanasundaram, K. *Photochemistry of Polypyridine and Porphyrin complexes*; Academic Press: New York, 1992.
(79) Nakae, Y.; Fukusaki, E.; Kajiyama, S.; Kobayashi, A.; Sakata, I. *J. Photochem. Photobiol., A.* **2005**, *171*, 91.
(80) Kruk, M. M.; Braslavsky, S. E. *J. Phys. Chem. A* **2006**, *110*, 3414.
(81) Kano, K.; Kitagishi, H.; Dagallier, C.; Kodera, M.; Matsuo, T.; Hayashi, T.; Hisaeda, Y.; Hirota, S. *Inorg. Chem.* **2006**, *45*, 4448.
(82) Bradshaw, J. E.; Gillogly; K, A.; Wilson, L. J.; Kumar, K.; Wan, X.; Tweedle, M. F.; Hernandez, G.; Bryant, R. G. *Inorg. Chim. Acta* **1998**, *275*−*276*, 106.
(83) Schaefle, N.; Sharp, R. *J. Phys. Chem. A* **2005**, *109* (15), 3267.
(84) Klein, A. T. J.; Rösch, F.; Coenen, H. H.; Qaim, S. M. *Appl. Radiat. Isot.* **2005**, *62*, 711.
(85) Itoh, J. I.; Yotsuyanagi, T.; Aomura, K. *Anal. Chim. Acta* **1975**, *74*, 53.
(86) Tabata, M.; Tanaka, M. *J. Chem. Soc., Chem. Commun.* **1985**, 42.
(87) Kalyanasundaram, K.; Neumann-Spallart, M. *J. Phys. Chem.* **1982**, *86*, 5163.
(88) Tabata, M.; Tanaka, M. *J. Chem. Soc., Dalton Trans.* **1983**, 1955.
(89) Tabata, M.; Ozutsumi, K. *Bull. Chem. Soc. Jpn.* **1992**, *65*, 1438.
(90) Zékány, L.; Nagypál, I. *Computational Methods for Determination of Formation Constants*; Legget, O. J., Ed.; Plenum Press: New York, 1985; Chapter 8.
(91) Zékány, L.; Nagypál, I.; Peintler, G.; PSEQUAD for Chemical Equilibria, Technical Sofware distributors, 1991.
(92) Zékány, L.; Nagypál, I.; Peintler, G.; *Manual for PSEQUAD*, Version 5.01; University of Szeged and University of Debrecen: Hungary, 2001.
(93) Peintler, G.; Nagypál, I.; Jancsó, A.; Epstein, I. R.; Kustin, K. *J. Phys. Chem.* **1997**, *101*, 8013.
(94) Peintler, G. *A Comprehensive Program Package for Fitting Parameters of Chemical Reaction Mechanisms*, reference manual ZITA, version 4.1; Attila József University: Szeged, Hungary, 1997.
(95) Rabek, J. F. *Experimental methods in photochemistry and photophysics*; Wiley-Interscience; New York, 1982.
(96) Demas, J. N. *Excited state lifetime measurements*; Acedemic Press, Inc.: New York, 1983.
(97) Wilhelm, E.; Battino, R.; Wilcock, R. J. *Chem. Rev.* **1977**, *77*, 219.
(98) Murov, S. L. *Handbook of photochemistry*; Marcel Dekker: New York, 1973.
(99) Hohenberg, P.; Kohn, W. *Phys. Rev.* **1964**, *136*, B864.
(100) Kohn, W.; Sham, L. J. *Phys. Rev.* **1965**, A1133.
(101) *The challenge of d and f electrons*; Salahub, D. R., Zerner, M. C., Eds.; American Chemical Society: Washington, DC, 1989.
(102) *Density-Functional Theory of Atoms and Molecules*; Parr, R. G., Wang, W., Eds.; Oxford University Press: Oxford, 1989.
(103) Becke, A. *Phys. Rev.* **1988**, *A38*, 3098.
(104) Lee, C.; Yang, W.; Parr, R. G. *Phys. Rev.* **1988**, *B37*, 785.
(105) Becke, A. D. *J. Chem. Phys.* **1993**, *98*, 5648.
(106) Zhao, Y.; Schultz, N. E.; Truhlar, D. G. *J. Chem. Phys.* **2005**, *123*, 161103.
(107) Zhao, J.; Schultz, N. E.; Truhlar, D. G. *J. Chem. Theory Comput.* **2006**, *2*, 364.
(108) Dunning, T. H.; Hay, P. J. In *Modern Theoretical Chemistry*; Schaefer, H. F., III, Ed.; Plenum Press: New York, 1976; Vol. 3, p 1.
(109) Hay, P. J.; Wadt, W. R. *J. Chem. Phys.* **1985**, *82*, 270.
(110) Wadt, W. R.; Hay, P. J. *J. Chem. Phys.* **1985**, *82*, 284.
(111) Hay, P. J.; Wadt, W. R. *J. Chem. Phys.* **1985**, *82*, 299.
(112) Facelli, J. C. *J. Phys. Chem. B.* **1998**, *102*, 2111.
(113) Dunietz, B. D.; Dreuw, A.; Head-Gordon, M. *J. Phys. Chem. B* **2003**, *107*, 5623.
(114) Yamaki, T.; Nobusada, K. *J. Phys. Chem. A* **2003**, *107*, 2351.
(115) Bauernschmitt, R.; Ahlrichs, R. *Chem. Phys. Lett.* **1996**, *256*, 454.
(116) Casida, M.; Jamorski, C.; Casida, K. C.; Salahub, D. R. *J. Chem. Phys.* **1998**, *108*, 4439.
(117) Stratmann, R. E.; Scuseria, G. E.; Frisch, M. J. *J. Chem. Phys.* **1998**, *109*, 8218.

(118) Frisch, M. J.; Trucks, G. W.; Schlegel, H. B.; Scuseria, G. E.; Robb, M. A.; Cheeseman, J. R.; Montgomery, Jr. J. A.; Vreven, T.; Kudin, K. N., Burant, J. C.; Millam, J. M.; Iyengar, S. S.; Tomasi, J.; Barone, V.; Mennucci, B.; Cossi, M.; Scalmani, G.; Rega, N.; Petersson, G. A.; Nakatsuji, H.; Hada, M.; Ehara, M.; Toyota, K.; Fukuda, R.; Hasegawa, J.; Ishida, M.; Nakajima, T.; Honda, Y., Kitao, O.; Nakai, H.; Klene, M.; Li, X.; Knox, J. E.; Hratchian, H. P.; Cross, J. B.; Bakken, V.; Adamo, C.; Jaramillo, J.; Gomperts, R.; Stratmann, R. E.; Yazyev, O.; Austin, A. J.; Cammi, R.; Pomelli, C.; Ochterski, J. W.; Ayala, P. Y.; Morokuma, K.; Voth, G. A.; Salvador, P.; Dannenberg, J. J.; Zakrzewski, V. G.; Dapprich, S.; Daniels, A. D.; Strain, M. C.; Farkas, O.; Malick, D. K.; Rabuck, A. D.; Raghavachari, K.; Foresman, J. B.; Ortiz, J. V.; Cui, Q.; Baboul, A. G.; Clifford, S.; Cioslowski, J.; Stefanov, B. B.; Liu, G.; Liashenko, A.; Piskorz, P.; Komaromi, I.; Martin, R. L.; Fox, D. J.; Keith, T.; Al-Laham, M. A.; Peng, C. Y.; Nanayakkara, A.; Challacombe, M.; Gill, P. M. W.; Johnson, B.; Chen, W.; Wong, M. W.; Gonzalez, C.; Pople, J. A. *Gaussian 03*, revision E.01; Gaussian, Inc.: Wallingford, CT, 2004.

(119) Adler, A. D.; Longo, F. R.; Kampas, F.; Kim, J. *J. Inorg. Nucl. Chem.* **1970**, *32*, 2443.

(120) Adler, A. D.; Longo, F. R.; Varadi, V. *Inorg. Synth.* **1976**, *16*, 213.

(121) Baker, H.; Hambright, P.; Wagner, L. *J. Am. Chem. Soc.* **1973**, *95*, 5942.

(122) Hambright, P.; Chock, P. B. *J. Am. Chem. Soc.* **1974**, *96*, 3123.

(123) Shamim, A.; Hambright, P. *Inorg. Chem.* **1980**, *19*, 564.

(124) Robinson, L. R.; Hambright, P. *Inorg. Chim. Acta* **1991**, *185*, 17.

(125) Sutter, T. P. G.; Hambright, P. *Inorg. Chem.* **1992**, *31*, 5089.

(126) Self, R. H.; Hambright, P. *J. Porphyrins Phthalocyanines* **2000**, *4*, 256.

(127) Shannon, R. D. *Acta Crystallogr.* **1976**, *A32*, 751.

(128) Adeyemo, A.; Krishnamurthy, M. *Inorg. Chim. Acta* **1984**, *83*, L41.

(129) Adeyemo, A.; Krishnamurthy, M. *Inorg. Chem.* **1977**, *16*, 3355.

(130) Tabata, M.; Nishimoto, J.; Ogata, A.; Kusano, T.; Nahar, N. *Bull. Chem. Soc. Jpn.* **1996**, *69*, 673.

(131) Nahar, N.; Tabata, M. *J. Porphyrins Phthalocyanines* **1998**, *2*, 397.

(132) Stone, A.; Fleischer, E. B. *J. Am. Chem. Soc.* **1968**, *90*, 2735.

(133) Thompson, A. N.; Krishnamurthy, M. *J. Inorg. Nucl. Chem.* **1979**, *41*, 1251.

(134) Butler, R. N. *Chem. Rev.* **1984**, *84*, 249.

(135) Funahashi, S.; Inada, Y.; Inamo, M. *Anal. Sci.* **2001**, *17*, 917.

(136) Inada, Y.; Sugimoto, Y.; Nakano, Y.; Funahashi, S. *Chem. Lett.* **1996**, 881.

(137) Kilian, K.; Pyrzynska, K. *Talanta* **2003**, *60*, 669.

(138) Ostfeld, D.; Tsutsui, M. *Acc. Chem. Res.* **1974**, *7*, 52.

(139) Hudson, M. F.; Smith, K. M. *Tetrahedron Lett.* **1974**, *26*, 2227.

(140) Platt, J. R. *J. Opt. Soc. Am.* **1953**, *43*, 252.

(141) Gouterman, M. *J. Chem. Phys.* **1959**, *30*, 1139.

(142) Gouterman, M.; Wagnière, G. H.; Snyder, L. C. *J. Mol. Spectrosc.* **1963**, *11*, 108.

(143) Ricciardi, G.; Rosa, A.; van Gisbergen, S. J. A.; Baerends, E. J. *J. Phys. Chem. A* **2000**, *104*, 635.

(144) Stone, A.; Fleischer, E. B. *J. Am. Chem. Soc.* **1968**, *90*, 2735.

(145) Thompson, A. N.; Krishnamurthy, M. *J. Inorg. Nucl. Chem.* **1979**, *41*, 1251.

(146) Shelnutt, J. A. *J. Phys. Chem.* **1984**, *88*, 4988.

(147) Bütje, K.; Nakamoto, K. *Inorg. Chim. Acta* **1990**, *167*, 97.

(148) Erdem, S. S. *J. Porphyrins Phthalocyanines* **1998**, *2*, 61.

(149) Vasil'ev, V. V.; Borisov, S. M.; Maldotti, A.; Molinari, A. *J. Porphyrins Phthalocyanines* **2003**, *7*, 780.

(150) Shelnutt, J. A. *J. Porphyrins Phthalocyanines* **2001**, *5*, 300.

(151) Darwent, J. R.; Douglas, P.; Harriman, A.; Porter, G.; Richoux, M.-C. *Coord. Chem. Rev.* **1982**, *44*, 83.

(152) Baskin, J. S.; Yu, H. Z.; Zewail, A. H. *J. Phys. Chem. A.* **2002**, *106*, 9837.

(153) Harriman, A. *J. Chem. Soc., Faraday Trans. 1* **1980**, *76*, 1978.

(154) Seybold, P.; Gouterman, M. *J. Mol. Spectrosc.* **1969**, *31*, 1.

(155) Gouterman, M.; Stryer, L. J. *Chem. Phys.* **1962**, *37*, 2260.

(156) Kunkely, H.; Horváth, O.; Vogler, A. *Coord. Chem. Rev.* **1997**, *159*, 85.

(157) Harriman, A. *J. Chem. Soc., Faraday Trans. 1* **1981**, *77*, 369.

(158) Bajema, L.; Gouterman, M.; Rose, C. B. *J. Mol. Spectrosc.* **1971**, *39*, 421.

(159) Gouterman, M. *J. Chem. Phys.* **1960**, *33*, 1523.

(160) Bonnet, R.; Ridge, R. J.; Land, E. J.; Sinclair, R. S.; Tait, D.; Truscott, T. G. *J. Chem. Soc., Faraday Trans. 1* **1982**, *78*, 127.

(161) Engst, P.; Kubát, P.; Jirsa, M. *J. Photochem. Photobiol., A* **1994**, *78*, 215.

(162) Kubát, P.; Mosinger, J. *J. Photochem. Photobiol., A.* **1996**, *96*, 93.

(163) Wen, T. C.; Hwang, L. C.; Lin, W. Y.; Chen, C. H.; Wu, C. H. *Chem. Phys.* **2003**, *286*, 293.

(164) Prendergast, K.; Spiro, T. G. *J. Phys. Chem.* **1991**, *95*, 9728.

(165) Oliver, F. W.; Thomas, C.; Hoffman, E.; Hill, D.; Sutter, T. P. G.; Hambright, P.; Haye, S.; Thorpe, A. N.; Quoc, N.; Harriman, A.; Neta, P.; Mosseri, S. *Inorg. Chim. Acta* **1991**, *186*, 119.

(166) Zerner, M.; Gouterman, M. *Inorg. Chem.* **1966**, *5*, 1707.

(167) Kuznetsova, N. A.; Okunchikov, V. V.; Derkacheva, V. M.; Kaliya, O. L.; Lukyanets, E. A. *J. Porphyrins Phthalocyanines* **2005**, *9*, 393.

(168) Ogunsipe, A.; Nyokong, T. *J. Porphyrins Phthalocyanines* **2005**, *9*, 121.

(169) Smith, K. M.; Lai, J. J. *Tetrahedron Lett.* **1980**, *21*, 433.

(170) Szulbinski, W.; Strojek, J. W. *J. Electroanal. Chem.* **1988**, *252*, 323.

(171) Evans, B.; Smith, K. M.; Cavaleiro, J. A. S. *J. Chem. Soc., Perkin Trnas. 1* **1978**, 768.

(172) Smith, K. M.; Brown, S. B.; Troxler, R. F.; Lai, J. J. *Tetrahedron Lett.* **1980**, *21*, 2763.

(173) Lai, J.-J.; Khademi, S.; Meyer, E. F., Jr.; Cullen, D. L.; Smith, K. M. *J. Porphyrins Phthalocyanines* **2001**, *5*, 621.

(174) Balch, A. L. *Coord. Chem. Rev.* **2000**, *200−202*, 349.

(175) Horváth, O.; Ford, P. C.; Vogler, A. *Inorg. Chem.* **1993**, *32*, 2614.

(176) Spikes, J. D. *Photochem. Photobiol.* **1992**, *5*, 797.

(177) Tokumaru, K. *J. Porphyrins Phthalocyanines* **2001**, *5*, 77.

(178) (a) Mayer, I. *Chem. Phys. Lett.* **1983**, *97*, 270. (b) Mayer, I. *Chem. Phys. Lett.* **1985**, *117*, 396 (addendum).

(179) (a) Mayer, I. *Int. J. Quantum Chem.* **1986**, *29*, 73. (b) Mayer, I. *Int. J. Quantum Chem.* **1986**, *29*, 477.

(180) Mayer, I. *J. Comput. Chem.* **2007**, *28*, 204.

(181) Oliveira, K. M. T.; Trsic, M. *J. Mol. Struct.-Theochem* **1999**, *464*, 289.

(182) Baerends, E. J.; Ricciardi, G.; Rosa, A.; van Gisbergen, S. J. A. *Coord. Chem. Rev.* **2002**, *230*, 5.

(183) Song, X.; Jentzen, W.; Jia, S.-L.; Jaquinod, L.; Nurco, D. J.; Medforth, C. J.; Smith, K. M.; Shelnutt, J. A. *J. Am. Chem. Soc.* **1996**, *118*, 12975.

(184) Jentzen, W.; Unger, E.; Song, X.-Z.; Jia, S.-L.; Turowska-Tyrk, I.; Schweitzer-Stenner, R.; Dreybrodt, W.; Scheidt, W. R.; Shelnutt, J. A. *J. Phys. Chem. A* **1997**, *101*, 5789.

JP804039S